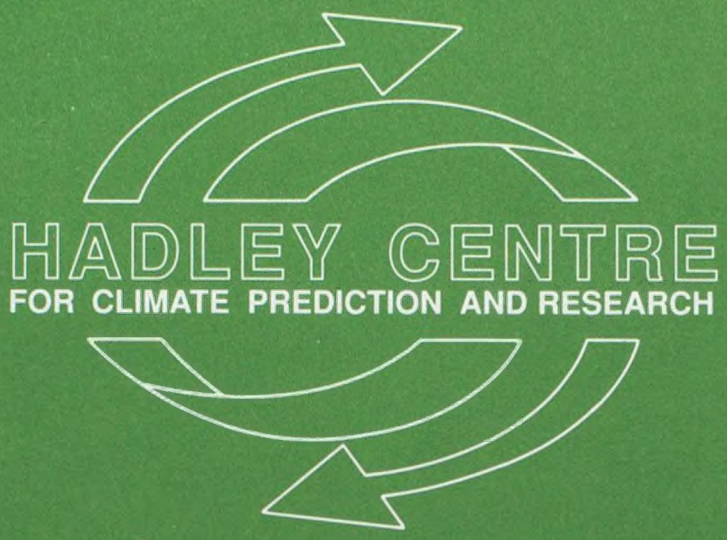

A Stratosphere - Troposphere Data Assimilation System

by

R. Swinbank and A. O'Neill

CRTN 35 March 1993

CLIMATE
RESEARCH
TECHNICAL
NOTE

Hadley Centre
Meteorological Office
London Road
Bracknell
Berkshire RG12 2SY

Climate Research Technical Note No. 35

A Stratosphere - Troposphere Data Assimilation System

Richard Swinbank
and
Alan O'Neill

Hadley Centre for Climate Prediction and Research
Meteorological Office
London Road
Bracknell
Berkshire
RG12 2SY

Note: This paper has not been published. Permission to quote from it should be obtained from the Director of the Hadley Centre.

A Stratosphere-Troposphere Data Assimilation System

by Richard Swinbank and Alan O'Neill

Abstract

A data assimilation system has been developed at the UK Met Office to analyse the mix of observations available in the troposphere and stratosphere. The data assimilation system is based on the "Analysis Correction" scheme used at the Met Office for operational weather forecasting.

The assimilation system is currently being used to supply near real time analyses of meteorological fields from the troposphere and stratosphere to the Upper Atmosphere Research Satellite (UARS) Science Team. At this stage, these analyses are based on a similar set of observations to the operational analyses, so they provide an independent check of the UARS observations. In the stratosphere they are largely based on soundings from the NOAA polar orbiters.

Some results from the assimilation system are presented for periods in January and August 1992. They are compared with equivalent products from the National Meteorological Center (NMC). A particular study is made of the Arctic polar vortex in late January.

Future developments of the assimilation system are also described. First, the vertical domain of the model will be extended into the middle mesosphere, with some improvement in vertical resolution. Second, the system will be extended to assimilate data from UARS instruments in addition to the other observation types; these UARS data will include observations of temperatures, winds and long-lived chemical species.

1. Introduction

The aim of this paper is to describe the data assimilation system which has been developed at the UK Meteorological Office for the Upper Atmosphere Research Satellite (UARS) project. This assimilation system is a development of the system used at the Met Office for operational weather forecasting (Lorenc et al 1991). The aim of the assimilation project is to provide a self-consistent, three-dimensional 'movie' of the atmosphere, up to the lower mesosphere. A sequence of synoptic maps (or "analyses") is constructed from a heteorogeneous mixture of data. The assimilation scheme takes into account the asynoptic nature of the observations, and their known errors. The potential of the assimilation system is demonstrated by comparing selected results with independent analyses.

The Upper Atmosphere Research Satellite was launched on 12th September 1991. Its aim is to make a systematic investigation of the stratosphere and mesosphere by taking a range of meteorological and chemical measurements. To that end, UARS carries a wide range of instruments to measure temperature, winds, composition and energy input of the atmosphere.

The primary contribution of the Met Office to the UARS project is to assimilate observations of the middle atmosphere into a global atmospheric general circulation model. A conventional analysis scheme, such as that used at the Met Office to analyse SSU data (Bailey et al. 1992), produces synoptic maps from observations of a particular type. The aim of the present work is to set up a system that has the potential to analyse a heterogeneous set of observations both from UARS and also from a variety of other sources. This analysis problem is somewhat similar to that faced by operational weather forecasting centres; it has been tackled by adapting the Met Office's operational assimilation system (Lorenc et al., 1991).

Currently being assimilated are non-UARS data, derived primarily from operational satellite temperature soundings and radiosonde ascents. Some results from these analyses are presented in this paper. They are independent "correlative" data, which are being supplied daily to the UARS science team to help validate UARS measurements and for diagnostic studies.

In the near future, observations from selected UARS instruments will be assimilated in addition to the operational observations. It is planned that the UARS data to be assimilated will include observations of temperatures, winds and long-lived chemical species. This enhanced version of the assimilation system has not yet been implemented routinely, although development is well advanced.

The plan of this paper is as follows. In section 2, an outline of the stratosphere-troposphere data assimilation system is given. Sections 3 and 4 outline the numerical model and the assimilation scheme. Section 5 describes the modifications that have been made to the assimilation system, and documents the analyses produced so far. Preliminary comparisons of the temperature analyses with observations and independent analyses are presented in section 6. These analyses allow a three-dimensional picture to be built up of the stratospheric circulation. Section 7 comprises a synoptic study of the Arctic polar vortex in late January 1992. More detailed studies based on our analyses, in particular comparisons with UARS observations, will be made at a later date. Finally, in section 8, plans for future studies and developments of the assimilation are described.

2. Overview of the assimilation system

Figure 1 illustrates the main data flows in the assimilation system. It illustrates how observations are extracted from Met Office data banks, and then processed. The UARS data will be acquired in a similar manner. The main component of that observation processing is quality control, in which the observations are checked against forecast data. For the purposes of observation processing only, the observations are grouped into six-hourly batches, so each observation is checked against the model field from the nearest forecast time. Next the observations are assimilated into a numerical model, when they are assimilated at their time of observation. The system produces a set of synoptic analyses, together with statistical information to aid data and model validation. Most of the assimilation system is run on the Met Office Cray Y-MP supercomputer.

Non-UARS observations are extracted from the Met Office operational data banks, and copied to the Cray computer system for subsequent processing. The main type of observations used in the stratosphere are temperature soundings from the polar orbiter satellites operated by the National Oceanographic and Atmospheric Administration (NOAA). These soundings are layer-mean temperatures produced by the National Environmental Satellite Data and Information Service (NESDIS) from the original radiance measurements. Two sources of satellite data are used: firstly "SATEM" reports, which comprise satellite soundings at approximately 500 km horizontal resolution and levels up to 1 HPa; and secondly, higher resolution soundings, originally supplied at 250 km resolution up to 1 HPa, and from late 1991 at 120km resolution up to 0.4 HPa. The latter data could not be included in all the assimilations owing to problems with the new data formats. Another important set of data are radiosonde soundings of temperatures and winds; these are occasionally available up to about 10 HPa, though more typically up to around 50 HPa. Additional observation types include aircraft winds and temperatures, satellite cloud-track winds and surface observations of pressure.

The parallel step for UARS observations consists of acquistion of UARS data from the Central Data Handling Facility (CDHF) at NASA Goddard Space Flight Center, and their transfer to the Cray system. The UARS observations to be used by the assimilation are "level 3AT" data, which are profiles on UARS standard pressure levels calculated approximately every minute along UARS viewing tracks.

For both non-UARS and UARS data, data acquisition is followed by observation pre-processing, the main component of which is observation quality control. This uses the Bayesian method developed by Lorenc and Hammon (1988). Observations are checked against values taken from a numerical forecast, at the location of the observations; we refer to these forecast values as "background" data. On the basis of expected errors in the observation and the background data, a statistical test is carried out to assess the probability that each observation is grossly in error. Where the

calculated probability indicates that an observation is likely to be incorrect, it is flagged and not passed to the assimilation. For most observation types (though not for satellite soundings), the probability calculation also incorporates a "buddy check", so that if an independent set of observations are consistent with each other they are more likely to be accepted, even when they disagree with the forecast data. Thus, the observation pre-processing stage produces a file containing quality-controlled observations in a suitable format for input to the assimilation.

Next, the assimilation is run by integrating a numerical model of the atmosphere in data assimilation mode. As the model is being integrated forward in time, its fields are adjusted towards the observed data, so that the state of the numerical model is a realistic representation of the state of the atmosphere to within the assumed errors. To produce background fields for quality control, the same model may also be run in forecast mode, in which case the evolution of the model state is governed solely by the model equations. The numerical model is described in section 3, and the assimilation scheme used with it, the Analysis Correction scheme, is described in section 4.

The assimilation step is illustrated in Figure 2. The central arrow represents the integration of the numerical model. The model is run for twenty-four hours in data assimilation mode, immediately followed by twenty-four hours in forecast mode. At the end of the assimilation period the model writes out a set of analysed fields interpolated to pressure levels. The levels are UARS standard pressure levels, which are equally spaced in log pressure, with six levels per factor of 10 in pressure, from 1000 HPa to 0.32 HPa. At the same time, a copy of the complete model state is taken as initial data for the next 24 hours of assimilation. Additional model fields are written out every six hours for use by the observation processing. The fields written out during the forecast period, denoted by 'B' in Fig 2, are used to quality-control the observations in the next day's run. The fields written out during the assimilation period, 'A' in Fig 2, are used during the observation post-processing, which is now described.

During the second phase of the observation processing an "Observation Processing Dataset" (or OPD) is compiled. The OPD is a major resource for validation of both the observations and the assimilation process. For each observation, the OPD stores the observed value, its difference from the analysis value (co-located with the observation), and also its difference from the background value. These differences may be used for routine monitoring and subsequent statistical analysis. For example, the mean observation minus background difference should be close to zero; if not, it indicates that there is a bias either in the model or in the relevant set of observations. Statistics generated daily from these differences give valuable information to users about the quality of the analyses.

The daily analysed fields from the assimilation stage are transferred to the UARS CDHF, where they are made available to other members of the UARS Science Team. Copies are also retained at the Met Office for further study.

3. Numerical Model

The numerical model used by the stratospheric assimilation system is the Met Office's "Unified Model" (UM). It was designed for a variety of applications, including operational weather forecasting and climate simulations. A split-explicit, conservative, finite-difference scheme is used for the dynamics (Cullen et al., 1991). The model incorporates a comprehensive set of physical parametrization schemes.

For our application, a stratosphere-troposphere configuration of the model is used. The model uses a regular latitude-longitude (Arakawa B) grid with a north-south resolution of 2.5° and an east-west resolution of 3.75°. This grid is the same as the one used for climate simulations, and is three times coarser than that used for operational forecasting. An advection timestep of 20 minutes is currently used, with three dynamics adjustment steps per advection step. The advection step is the timestep used by the physical parametrizations. A hybrid vertical coordinate system is used: the levels are terrain-following near the ground, but gradually become constant pressure surfaces higher up (Fig 3). Currently, there are 42 levels, with a vertical resolution in the stratosphere of approximately 1.6 km (10 levels per factor of 10 in pressure); the top level of the model is at 0.28 HPa.

In this configuration, the standard radiation scheme (Ingram, 1992) was unsatisfactory at high levels, largely because it was designed for tropospheric conditions. So some amendments were made to the parametrization of long-wave radiation, based on the ECMWF scheme (Morcrette et al., 1986); amendments to represent the effects of Doppler line broadening have also been included. The gravity-wave drag scheme (Palmer et al., 1986), which was also developed for tropospheric models, introduced too much noise in the stratosphere. As a temporary expedient, it was replaced in the upper stratosphere and lower mesosphere by a simple Rayleigh friction scheme, which was adapted from the Met Office stratosphere-mesosphere model (Fisher, 1987).

4. Assimilation Scheme

The aim of a meteorological analysis scheme is to construct a synoptic field which comprises an optimum combination of all available information. In addition to fitting observations at a particular time, the analysis should also use information from previous observations; this

information is taken into account using background data from forecasts with a numerical model.

The UARS assimilation system uses the Met Office's operational assimilation scheme, known as the "Analysis Correction" (or AC) scheme, which has been described by Lorenc et al (1989, 1991). Since the original implementation, it has been adapted for use in conjunction with the Unified Model (Bell et al, 1991). At the same time, some changes were made to the vertical analysis of satellite data; these are outlined at the end of this section, since they are of particular relevance to stratospheric analyses.

The Analysis Correction scheme is a modified version of the successive correction method of data assimilation. It incorporates repeated insertion of data, in which the model is gradually adjusted to new observational data so that a measure of dynamical balance is retained. This ensures that slowly varying modes of the model are preferred; these generally correpond to the atmospheric motions that we wish to analyse and forecast. Prior knowledge about atmospheric structures is incorporated in the analysis procedure by imposing a degree of geostrophic balance and non-divergence of wind increments.

As a simple illustration of the principle of data assimilation, consider the optimum combination of two independent observations x_1, x_2 of the same quantity x. Assume the two observations are each taken from Gaussian distributions with standard deviations σ_1 and σ_2. The best estimate of x (in a 'least squares' sense) is given by

$$\langle x \rangle = \{x_1/\sigma_1^2 + x_2/\sigma_2^2\} / \{1/\sigma_1^2 + 1/\sigma_2^2\} \qquad (4.1)$$

The less accurate the observation, the less weight it is given.

One can obtain the same result by choosing x so as to minmise a 'penalty function' J which quantifies the fit of possible values of x to the observations x_1, x_2

$$J(x) = (x-x_1)^2/\sigma_1^2 + (x-x_2)^2/\sigma_2^2 \qquad (4.2)$$

Large differences of x from accurate observations give large contributions to J. The best estimate is at the minimum of J, and equals <x> (Eq 4.1).

For the more complex meteorological analysis problem, one can construct a similar penalty function which quantifies the fit of the analysis $\mathbf{x}$ to the observations $\mathbf{y_o}$ and to the model background $\mathbf{x_b}$. ($\mathbf{x}$ and $\mathbf{x_b}$ are column vectors corresponding to each analysed variable at each grid point, and $\mathbf{y_o}$ is a column vector comprising all the observed parameters in every observation).

$$J = (y_o - K(x))^* O^{-1} (y_o - K(x)) + (x_b - x)^* B^{-1} (x_b - x) \quad (4.3)$$

Here **O** is the observation error covariance matrix, **B** is the background error covariance matrix, **K** represents the interpolation between analysis grid-points and observation locations and the symbol * denotes transpose. The aim is to construct an optimum analysis <x> which minimises the penalty function J.

Because the matrices in Eq. (4.3) are very large, it is impracticable to find the exact minimum of J. Instead a descent algorithm is used to approach the optimum analysis iteratively, whereby the u'th estimate x_u of the optimum analysis is used to derive an improved estimate x_{u+1}. We use a simple Newton-Raphson method:

$$x_{u+1} = x_u - \lambda (J'')^{-1} J' \quad (4.4)$$

where **J'** is a column vector of the partial derivatives of J (with respect to the components of **x**), and **J''** (the Hessian matrix) is a square matrix of second derivatives of J with respect to the components of **x**. The scalar constant λ is a relaxation factor which controls the step-size of the iteration. Each iteration moves the estimate down the gradient of J towards the optimum analysis, as illustrated in Fig 4.

After some manipulation (see Lorenc et al., 1991), Eq. (4.4) leads to the equation

$$x_{u+1} = x_u + \lambda Q \{W(y_o - K(x_u)) + (x_b - x_u)\} \quad (4.5)$$

where **W** is a matrix of weights and **Q** is a matrix of normalisation factors:

$$W = BK^* O^{-1} \quad (4.5a)$$

$$Q = (WK + I)^{-1} \quad (4.5b)$$

Equation 4.5 shows that on each each iteration the previous estimate of the analysis is corrected by a weighted sum of the discrepancies with the observations and the background field.

The following approximations convert Eq. (4.5) to the Analysis Correction scheme. First, the background term $(x_b - x_u)$ is omitted. Second, Eq (4.5) is not iterated to convergence; information from the background field is retained by starting from x_b. Despite the omission of the term $(x_b - x_u)$, the analysis **x** will not differ much from x_b where the background is much more accurate than the observations. Third, in order to improve the convergence of the algorithm when there are variations in observation density, **Q** is replaced by a modifed form evaluated at observation points rather than analysis grid points. The iteration equation is thus

$$\mathbf{x}_{u+1} = \mathbf{x}_u + \lambda \mathbf{W Q} (\mathbf{y_o} - \mathbf{K}(\mathbf{x}_u)) \quad (4.6)$$

For further discussion and justification of these approximations, see Lorenc et al (1991).

The matrix **BK*** is modelled by a continuous function of the form:

$$(BK^*)_{ij} = B_{ii}\, \mu(h_{ij})\, \eta(v_{ij}) \quad (4.7)$$

where μ and η are continuous functions of the horizontal distance h_{ij} and vertical distance v_{ij} between the observation points i and the model grid points j. The function μ is a second-order autoregressive function with a prescribed horizontal correlation scale s:

$$\mu(h_{ij}) = (1 + h_{ij}/s) \exp(-h_{ij}/s) \quad (4.8)$$

In order to allow the model to adjust to each observation, it is assimilated with increasing weight for five hours before its observation time, with full weight at its observation time, and with decreasing weight for one hour afterwards. This is achieved by amending Eq (4.6) as follows:

$$\mathbf{x}_{u+1} = \mathbf{x}_u + \lambda \mathbf{W Q}\ \mathbf{R} (\mathbf{y_o} - \mathbf{K}(\mathbf{x}_u)) \quad (4.9)$$

where **R** is a diagonal matrix of time factors, and where $\mathbf{y_o}$ incorporates observations in a six-hour time window. Lorenc et al. (1991) give further details of this modification. In practice, a single analysis iteration is made for each time-step of the model. Over a period, this is equivalent to going through several cycles of iteration, in so far as the states of the atmosphere and the model are slowly varying.

It can be shown from Eq. (4.9) that the calculation of increments $\mathbf{x}_{u+1} - \mathbf{x}_u$ can be broken into separate analysis steps, as illustrated in Fig 5. First, surface pressure observations are analysed. The increments to the model pressure field are calculated from Eq 4.9. Since there is a correlation between surface pressure and other meteorological fields (at least at low levels), the temperature and wind fields are adjusted hydrostatically and geostrophically to take into account the change in surface pressure. Second, temperature data are analysed, and further geostrophic increments added to the wind fields to take into account the implied change in geopotential height of constant pressure surfaces. Third, wind observations are analysed and non-divergent increments added to the model fields. Fourth, relative humidity data are analysed (in the troposphere only). After one iteration of the analysis has been completed, the general circulation model is integrated forward by one (advection) time-step.

The temperature sounders on board the NOAA polar orbiters have rather low vertical resolution, so retrieved temperatures are reported as layer-mean values, which are directly related to layer thicknesses. However, many other assimilation schemes, including an earlier version of the AC scheme, treat such temperatures as point values, in a similar manner to temperature profiles from radiosondes. Such an approach is inconsistent with the data and leads to problems when attempting to assimilate satellite and radiosonde data together. By contrast we treat the measurements correctly as layer thicknesses. The model temperature fields are adjusted so that the geopotential difference (thickness) between a pair of pressure levels in the model is consistent with the reported satellite layer-mean tempertures. This allows the analysis to incorporate information on finer vertical scales from radiosondes and yet remain consistent with the satellite data.

The interpolation method illustrated in Fig 6. First, geopotential thicknesses are calculated from the model fields for the satellite observation layers. Since the UM is written in terms of potential temperature θ rather than temperature, the geopotential difference $\Delta\Phi$ across an observation layer is calculated from:

$$\Delta\Phi = \int c_p \, \theta \, d\Pi \qquad (4.10)$$

The symbol Π indicates the Exner function ($\Pi = (p/p_{ref})^{\kappa}$). This integral is indicated by the shaded region in Fig 6a. For partial model layers it is assumed that the potential temperature θ varies linearly with Π. The model-derived thickness is converted to a layer-mean temperature using the expression

$$T = \Delta\Phi \, / \, (R \, \Delta\log(p)) \qquad (4.11)$$

as indicated by the shaded region in Fig 6b. The model-derived temperature is compared with the reported layer-mean temperature to give a temperature correction.

The temperature corrections (δT) for the satellite layers are then converted back to potential temperature corrections ($\delta\theta$) for the corresponding model layers. The required change to the geopotential thickness ($\delta\Phi$) for a model layer is given by:

$$\delta\Phi = \int R \, \delta T \, d(\log(p)) \qquad (4.12)$$

This integral is indicated by the shaded region in Fig 6c. Hence, an adjustment to the potential temperature at each model layer is calculated (as shown by the shaded region in Fig 6d):

$$\delta\theta = \delta\Phi / (c_p \Delta\Pi) \qquad (4.13)$$

The potential temperature adjustments at the locations of the satellite soundings are then used to calculate θ increments at model grid points, by applying Eq (4.9). A more detailed account of the interpolation method is given by Swinbank and Wilson (1990).

5. The Stratosphere-Troposphere analyses

The model configuration used for the stratosphere-troposphere assimilation system uses twice the timestep and three times the horizontal grid length of the operational model. It is designed to produce optimum analyses in the stratosphere, wheras the operational system is primarily designed for the troposphere. In view of these differences, the assimilation parameters used for the stratospheric assimilation are amended from those used by the operational system; the main parameters are summarised in Table 1. Note that a longer horizontal correlation scale is used in the UARS system, and geostrophic wind increments are used to balance temperature increments in the stratosphere, rather than being reduced to zero at upper levels. These changes were made following preliminary experimentation (Swinbank 1990).

A preliminary version of the stratosphere-troposphere assimilation system was used to analyse data for January 1991, as a pilot study before the launch of UARS. After the launch of UARS, regular near real-time assimilations were started in October 1991, based on operational observations. They are primarily intended to comprise a source of independent, or "correlative", analyses for the UARS project. Table 2 details the major changes made to the assimilation system since the start of the correlative assimilation runs.

During the first few months, the correlative analyses had some problems at high levels. The model was generating sharp temperature gradients in the top-most levels, which gradually penetrated lower down. This led to a failure in the assimilation in mid-December 1991. The problems were overcome by introducing some Rayleigh friction into the upper levels, assimilating satellite soundings up to 0.4 HPa (previously only data up to 1 HPa had been available) and tuning the quality control scheme so that satellite soundings were less likely to be rejected. The assimilations were re-started at the end of January, and there have been no major failures since then. The gap between mid-December and the end of January has since been filled with delayed-mode assimilations.

The Met Office stratosphere-troposphere analyses are currently available to other UARS investigators via the UARS CDHF. It is planned that they will also eventually be available to users in th UK via the Geophyical Data Facility (GDF) at the Rutherford Appleton Laboratory.

6. Temperature analyses

The analyses produced by the stratosphere-troposphere data assimilation system will be used for a variety of diagnostic studies of the middle atmosphere. In this and the following sections, some preliminary results are presented. This section focuses on the analysis of temperature observations in winter in both the northern hemisphere and southern hemisphere. The temperature analyses are singled out for study because the vast majority of stratospheric observations that are assimilated are temperature soundings.

The analyses are compared with the equivalent analyses produced by the US National Meteorological Center (NMC). The NMC analyses are used by several UARS investigators to compare with measurements from UARS instruments. The NMC analyses are a product of their operational data assimilation at lower levels (up to 100 HPa), while the upper level fields (70 HPa and above) are generated by a separate stratospheric analysis of thickness and temperatures based on NOAA satellite data and radiosonde data (up to 10 HPa, where available); the analysis procedure is described in Geller et al (1983). A more comprehensive comparison of the Met Office correlative analyses with the NMC product is currently in preparation (Manney et al., 1993).

In addition, the correlative analyses have been compared with various other analyses. They include the Met Office analysis of data from the Tiros Operational Vertical Sounders (TOVS) and Stratospheric Sounding Units (SSU) on the NOAA satellites; for brevity we refer to these analyses as the SSU analyses. The SSU analysis system is described by Bailey et al (1992). Like the NMC analyses, the Met Office SSU analyses are a combination of operational analyses up to 100HPa, and a separate analysis of thickness data at higher levels.

The results presented in this section concentrate on the analyses of temperature data for 9 January and 10 August 1992. The two dates were chosen because they are both within periods chosen by the UARS science team for the intercomparison of UARS data with analyses and with independent observations. Broadly speaking, the results are representative of other days studied in the northern and southern winter periods.

Figure 7 shows the zonally-averaged temperatures from our (UKMO) analyses for 9 January, together with the differences between the UKMO and NMC temperatures (UKMO-NMC). In the troposphere and lower stratosphere the temperature differences are generally small (typically less than 1 K). Near the South Pole the differences are rather larger; at low levels they are attributable to differences in the treatment of

high Antarctic topography, but there are also some significant differences of about 4 K up to 100 HPa.

The main difference between analyses are in the upper stratosphere. Moreover, there seems to be a coherent vertical structure in the difference field: UKMO zonal-mean temperatures are generally about 5 K warmer than NMC's near the stratopause (about 1-2 HPa), and are colder above and below. This difference is consistent with, though smaller than, the known bias in the NMC analyses near the stratopause (Finger et al., 1992). A tentative explanation of the differences between UKMO and NMC is that the NMC analysis scheme uses the TOVS soundings as point temperatures rather than layer-mean temperatures, while the UKMO scheme treats the temperature data more correctly (see section 4). These remarks do not necessarily imply that the UKMO temperatures are more trustworthy than NMC's in the upper stratosphere, since the numerical model has errors which have yet to be fully characterised. In particular, the large temperature differences near the stratopause over the Noth Pole are attributable, at least in part, to numerical errors in the model generated by a cross-polar flow; on other dates where cross-polar flow did not occur the differences near the North Pole were much more similar to those found at other latitudes.

Figures 8, 9 and 10 are synoptic maps of temperature at 12 GMT on 9 January 1992 for 100, 10 and 1 HPa for both UKMO and NMC analyses. At 100 HPa the agreement is very good, reflecting the comparatively rich observational coverage. At this level the NMC analyses are from their operational assimilation system. At 10 HPa the large-scale features of both maps are in broad agreement. Both show a pronounced 'wave 1' pattern, with good agreement in the positions of the main warm and cold areas. The UKMO-NMC difference map for 10 HPa is plotted in Fig 11; this shows more clearly that there are some large temperature differences, of more than 10 K over Europe and western Asia. Figure 10 compares the analyses at 1 HPa. Once again, the broad scale patterns are similar but there are some large local temperature differences. In general, the NMC stratospheric analyses are much smoother than their Met Office counterparts, with less extreme maxima and minima (after allowing for any systematic differences). Much of the small-scale structure in the UKMO temperatures is likely to be 'noise'. At 1 HPa, the analysis level is getting close to the top of the assimilation model, and the model is more subject to errors than lower down; any soundings that are several degrees in error are more likely to be passed by the quality control scheme and fitted by the assimilation.

Figure 12 shows zonal mean temperature cross-sections for August 10th. In some respects they are similar to the corresponding plots for 9 January (Fig 7). The Met Office analyses are again significantly warmer near the stratopause, and colder above. At around 10 HPa the Met Office analyses are significantly colder than NMC in the southern hemisphere, particularly near 75°S. It is possible that these differences at high latitudes

stem from model errors when representing strong winds in the neighbourhood of the poles, as found for 9 January.

Figure 13 shows the Met Office 10 HPa field for 10 August, together with the (UKMO-NMC) differences. It is clear that the Met Office analyses are consistently about 2 K colder than NMC through the whole southern hemisphere. Although Finger et al. (1992) do not quote a value for the NMC temperature bias at 10 HPa (because radiosonde data are included when they are available), it is possible that there is a positive bias of about 2 K in the NMC data in the southern hemisphere. The differences at high latitudes are up to 12 K in localised regions. Similar plots showing the difference with the ECMWF 10 HPa analysis are in Fig 14. In this case the difference is in the opposite sense; the ECMWF analysis of the polar vortex is colder than the Met Office analysis, by a similar amount that the Met Office analysis is colder than NMC. This level is right at the top of the domain of the ECMWF analysis (so it should not be expected to be of high quality), but the comparison illustrates the degree of uncertainty of the temperature in the polar vortex at 10 HPa.

An independent estimate of any bias in the Met Office analyses may be obtained by using the data stored in the OPD. Figures 15a and 15b are respectively graphs of observation minus analysis (O-A) and observation minus background (O-B) values from the OPD. The graphs summarise statistics for all satellite temperature soundings during the period 15 GMT 9 August to 15 GMT 10 August. The central graph shows the global mean O-A (or O-B) values, divided into pressure layers, and the dashed lines show the mean plus or minus the standard deviations. The O-A graphs shows that the analyses fit the observations, to within a small bias of magnitude less than 0.2K (depending on the layer). The standard deviation varies from around 1 K below 10 HPa to around 2 K above 1 HPa. Thus the statistics show that the analyses fit the observations to within the expected observation accuracy, with only a small bias. The O-B graphs indicate that the forecast fields have a significant bias, which is corrected by the assimilation. The OPD data may also be divided into latitude bands; Figure 16 shows similar OPD graphs for all data south of 30°S. The O-B graphs show that there is a clear systematic model error in the southern hemisphere extra-tropics (which needs to be addressed by future model developments). However, the O-A graphs show that the assimilation removes virtually all the bias which was present in the forecast; this confirms that the analyses are not significantly biased, at least as far as layer-mean temperatures are concerned. The fit to temperature observations is less good in this case than shown by the global statistics.

7. The Arctic polar vortex

Now we illustrate the use of the analyses with a brief case study of the three-dimensional structure of the polar vortex during a meteorologically interesting period in late January 1992. An unusally

persistent blocking ridge in the upper troposphere over the Atlantic and north-west Europe occurred during the winter of 1991/2. This led to pronounced anomalies in the pattern of flow in the lower stratosphere, and in turn to a deep minimum in the total column amount of ozone which was positioned over the tropospheric anticylone (Farman et al, 1993). The blocking was maintained (with some fluctuation in strength and position) for most of December, January and early February. The blocking system raised isentropic surfaces above it, and the cold core of the vortex at upper levels moved towards the European sector, to lie above the blocking system. In the lower stratosphere, the lowest temperatures shifted from near the centre of the polar vortex, where winds are weak, into the jet stream.

We focus on the three-dimensional structure of the polar vortex on 27 January 1992. This day shows many of the most important features of the 1991/2 winter-time circulation, and the structure of the vortex has particular interest. Figure 17 shows the temperatures in a cross-section on the plane of the Greenwich meridian, viewed from the western hemisphere. The lowest extra-tropical temperatures are located above 65°N, 0°E. Figure 18 shows the wind speed along the same section (solid lines lines indicate flow into the page, broken lines flow out of the page). There is a cyclonic vortex extending from the troposphere into the mesosphere. Its centre is shown by the zero-wind line near the middle of the figure. This line is not vertical, but shows a pronounced dislocation between 20 HPa and 10 HPa. The coldest air is not at the centre of the vortex but in the midde of the peripheral jet stream. By contrast, in the upper stratosphere a more normal arrangement of wind and temperature is seen: the lowest temperature is near the centre of the vortex (isotherms bow upwards along the zero-wind contour). Thus the centre of the vortex in the upper stratosphere lies vertically above the lowest temperatures in the lower stratosphere, which in turn lie above the blocking system in the tropsosphere. (This system is associated with the in-out-in pattern at the bottom right of Fig 18, and corresponds to the 'omega' pattern seen in Fig. 19). Isentropic surfaces bow upward in the cold air, so that air circulating round the vortex in the lower stratosphere cools as it rides over the top of the block, and later warms as it sinks back. Thus the tropospheric block has a marked effect on the temperature and wind in the lower stratosphere; widespread chemical processing (potentially leading to ozone depletion) could result from the displacement of the temperature minimum from the centre of the vortex into the jet stream.

In the upper stratosphere a notable feature in Fig 18 is the anticyclone on the flank of the polar vortex. This is the Aleutian High: there is a closed circulation around the zero-wind line at 10 HPa near 65°N, 180°E, which extends from about 50 HPa to about 3 HPa. Above, its presence is manifested as a bifurcation of the westerly jet stream, as shown by the local minmum in wind speed in middle latitudes. The bifurcation point lies roughly where the jet core would be in undisturbed conditions.

The vertical extension of The Aleutian High disrupts the flow in the upper stratosphere well within the vortex, a common feature in winter.

Isentropic potential vorticity (PV) maps for the upper troposphere (Fig 19, the 315K surface) and lower stratosphere (Fig 20, the 520K surface) futher illustrate the controlling influence of the lower flow. In the troposphere the blocking ridge corresponds to the pronouced poleward penetration (near 0° longitude) of low-PV air from lower latitudes. The ridge extends upwards into the lower stratosphere, as indicated by the 'kidney' shape in the distribution of high PV associated with the vortex. On higher surfaces the influence of the ridge fades and the flow becomes progressively more zonal. Downstream there is a pronounced extension of high PV air over Europe, indicating that air associated with the vortex is covering the region. That this air was chemically perturbed was confirmed by the elevated amounts of chlorine monoxide measured by Gerber and Kämpfer (1993) and by the MLS instrument on UARS (Waters, pers. comm.).

To the east of this extension lies a patch of high-PV air separated from the main body of the vortex. It has a vertical extent of about 10 km. A daily sequence of maps reveals that this air has been sliced from the vortex. It is not associated with a closed cyclonic circulation; rather it lies in a shear zone at the periphery of the vortex. This is a clear illustration (confirmed by independent analyses of PV constructed at ECMWF) of the irreversible mixing of air from the periphery of the vortex into mid-latitudes.

8. Future Plans

At present, the assimilation system is being extended to process UARS observations in addition to the operational data. Initially, temperature soundings from the Improved Stratospheric and Mesospheric Sounder (ISAMS) and the Microwave Limb Sounder (MLS) will be assimilated. These will be followed by stratospheric winds measured by the High Resolution Doppler Imager (HRDI); these data will allow the study of the impact of wind observations on dynamical diagnostics. Observations of long-lived chemical species from various UARS instruments will also be assimilated; the model tracer advection scheme will be used to carry this constituent data forward in time. The comparison of the analyses with UARS observations and results from the assimilation of UARS data will be the subject of subsequent papers.

It is also planned to improve the vertical resolution of the model. The domain of the model will be extended into the middle mesosphere, using 49 levels. The vertical resolution will be improved from about 1.6 km in the stratosphere to about 1.3km; at this resolution (12 levels per factor of 10 in pressure), alternate model levels will coincide with the UARS standard set of pressure levels. This will reduce vertical

interpolation errors in the analyses that are supplied to the UARS science team on standard UARS levels.

The results presented in this paper are only a foretaste of the studies that are planned. A more comprehensive intercomparison of analyses from this assimilation system and NMC is currently in preparation (Manney et al., 1993). In addition, dynamical topics such as stratospheric sudden warmings and stratosphere - troposphere interactions will be studied using these analyses. By studying the interplay of dynamics with chemical constituents, the UARS project will greatly enhance our understanding of the middle atmosphere, particularly as it relates to problems such as ozone depletion and climate change.

Acknowledgements

We would like to acknowledge the contributions of many people at the Met Office to the stratospheric data assimilation project. All of the middle atmosphere research group have contributed to the work to some degree, in particular Nigel Roberts, who adapted the operational observation processing programs, and Mike Bailey, who is responsible for the routine running of the assimilations. We also acknowledge the work done by Andrew Lorenc and his group, who developed the Analysis Correction data assimilation scheme, and Mike Cullen and the team that developed the Unified Model.

Table 1

Comparison of assimilation parameters for operational and stratospheric assimilations

Parameter		Operational	Stratospheric
No. model levels		20	42
Latitude grid spacing		0.8333°	2.5°
Longitude grid spacing		1.25°	3.75°
Model timestep		10 min	20 min
Relaxation factor λ	(NH)	0.35	
	(tropics)	0.2	
	(SH)	0.225	
	(mass)		0.36
	(wind)		0.48
Horizontal correlation scale s	(start)	360 km	500 km
	(ob time)	225 km	300 km
	(end)	250 km	300 km
Horizontal geostrophic adjustment weight	(NH)	0.5	0.7
	(SH)	0.7	0.7
Vertical geostrophic adjustment weight	(550+ HPa)	1.0	1.0
	(250 HPa)	0.2	0.3
	(100 HPa)	0.0	0.8

Note - in the stratospheric assimilation, the nudging coefficients are global figures, and operationally they are independent of observation type.
- the vertical geostrophic adjustment weights are specified at 50 HPa intervals; the comparisons in the table are for representative levels.
- the correlation scales shown above for the stratospheric analyses were subsequently increased from 500 and 300km to 750 and 500km respectively.

Table 2

Summary of UARS correlative assimilations, showing major changes

Dates	UM version	Comments
17 Oct 91 - 16 Dec 91	2.2	Start near real time correlative assimilation run. 20 minute advection time-step, with 2 adjustment steps per advection step. Satellite data only available up to 1 HPa. Assimilation failed on 17 Dec.
7 Dec 91 - 6 Jan 92	2.5	Delayed-mode run. Satellite data used up to 0.4HPa. Revised quality-control parameters. Daily climatology (ozone, sea surface temperatures, etc.) updating. Prevention of wave 1 filtering at poles. Rayleigh drag scheme incorporated. ECMWF-like changes to radiation scheme. Filtered orography. OPD available.
7 Jan 92 - 28 Jan 92	2.4	Delayed-mode run. Satellite data used up to 0.4 HPa. Revised quality-control parameters. Rayleigh drag scheme incorporated. OPD available.
7 Jan 92 - 11 Jan 92	2.5	Re-run, using second-order advection and prevention of filtering wave 1 at poles (else as previous run).
27 Jan 92 - 24 Feb 92	2.2	Near real-time run. Satellite data used up to 0.4 HPa. * Revised quality-control parameters. * Rayleigh drag scheme incorporated. * OPD available. *

25 Feb 92 - 26 May 92	2.4	Near real-time run. Daily update of climatological fields (e.g. ozone, sea surface temperatures) from 8 Apr 92 (previously done irregularly). *
27 May 92 - 25 Aug 92	2.5	Near real-time run. Prevention of wave 1 filtering at poles. * Filtered orography. * Use 3 (rather than 2) adjustment steps per advection step from 2 Aug 92.
26 Aug 92 - 17 Nov 92	2.6	Near real-time run. Output fields to include vertical velocity ω in addition to u, v, T, z.* From 17 Oct some assimilation parameters were changed (see note to Table 1).*
11 Nov 92 onwards	2.7	Near real-time run.

Note - * denotes changes that are included in the assimilations for all subsequent dates

References

M.J. Bailey, A. O'Neill and V.D. Pope (1992) Stratospheric analyses produced by the U.K. Meteorological Office. *J. Appl. Met.. (to appear).*

R.S. Bell, A.C. Lorenc, B. Macpherson and R. Swinbank (1991) The Analysis Correction Data Assimilation scheme. *Unified Model Documentation Paper 30. Available from S. Division, Met Office, UK.*

M.J.P. Cullen and T. Davies (1991) A conservative split-explicit integration scheme with fourth-order horizontal advection.*Q.J.R. Meteorol. Soc.*, **117**, 993-1002.

J.C. Farman, A. O'Neill and R. Swinbank (1993) The dynamics of the Arctic polar vortex during the EASOE campaign. *Geophys. Res. Lett. (to appear).*

F.G. Finger, M.E. Gelman, J.D. Wild, M.L. Chanin, A. Hauchecorne and A.J. Miller (1992) Evaluation of NMC upper stratospheric analyses using rocketsonde and lidar data. *submitted to Bull. Amer. Meteorol. Soc.*

M. Fisher (1987) The Met O 20 stratosphere-mesosphere model. *Dynamical Climatology Technical Note 52. Available from CR Divsion, Met Office UK.*

M.A. Geller, M.-F. Wu and M.E. Gelman (1983) Troposphere-stratosphere (surface-55km) monthly winter general circulation statistics for the Northern Hemisphere. *J. Atmos. Sci.*, **40**, 1334-1352.

L. Gerber and N. Kämpfer (1993) Millimeter-wave measurements of chlorine monoxide at the Junfraujoch alpine station. *Geophys. Res. Lett. (submitted).*

W.J. Ingram (1992) Radiation. *Unified Model Documentation Paper 23 Available from FR Division, Met Office, UK.*

A. C. Lorenc, R.S. Bell and B. Macpherson 1989 The new Meteorological Office data assimilation scheme. *Met O 11 Technical Note No. 27. Available from FR Division, Met Office, UK.*

A. C. Lorenc, R.S. Bell and B. Macpherson 1991 The Meteorological Office Analysis Correction Data Assimilation scheme. *Q.J.R. Meteorol. Soc.*, **117,** 59-89.

A.C. Lorenc and O. Hammon 1988 Objective quality control using Bayesian methods. *Q.J.R. Meteorol. Soc.*, **114,** 515-543.

G. Manney, R. Zurek, A. O'Neill, R. Swinbank, J. Miller and M. Gelman 1993 Intercomparison of NMC and UKMO analyses and derived products for UARS. *(in preparation; working title)*

J.-J. Morcrette, L.D. Smith and Y. Fouquart 1986 Pressure and temperature dependence of the absorption in longwave radiation parametrizations. *Beitr. Phys. Atmosph.*, **59,** 455-469.

T.N. Palmer, G.J. Shutts and R. Swinbank 1986 Alleviation of a systematic westerly bias in general circulation and numerical weather prediction models through an orographic gravity wave drag parametrization. *Q. J. R. Meteorol. Soc.*, **112,** 1001-1039.

R. Swinbank and C.A. Wilson 1990 Vertical interpolation of temperature observations and model data. *Short-Range Forecasting Research Technical Note No. 48. Available from FR Division, Met Office, UK.*

R. Swinbank 1990 Stratospheric Analysis Experiments with a 20-level sigma-coordinate model. *Short-Range Forecasting Research Technical Note No. 43. Available from FR Division, Met Office, UK.*

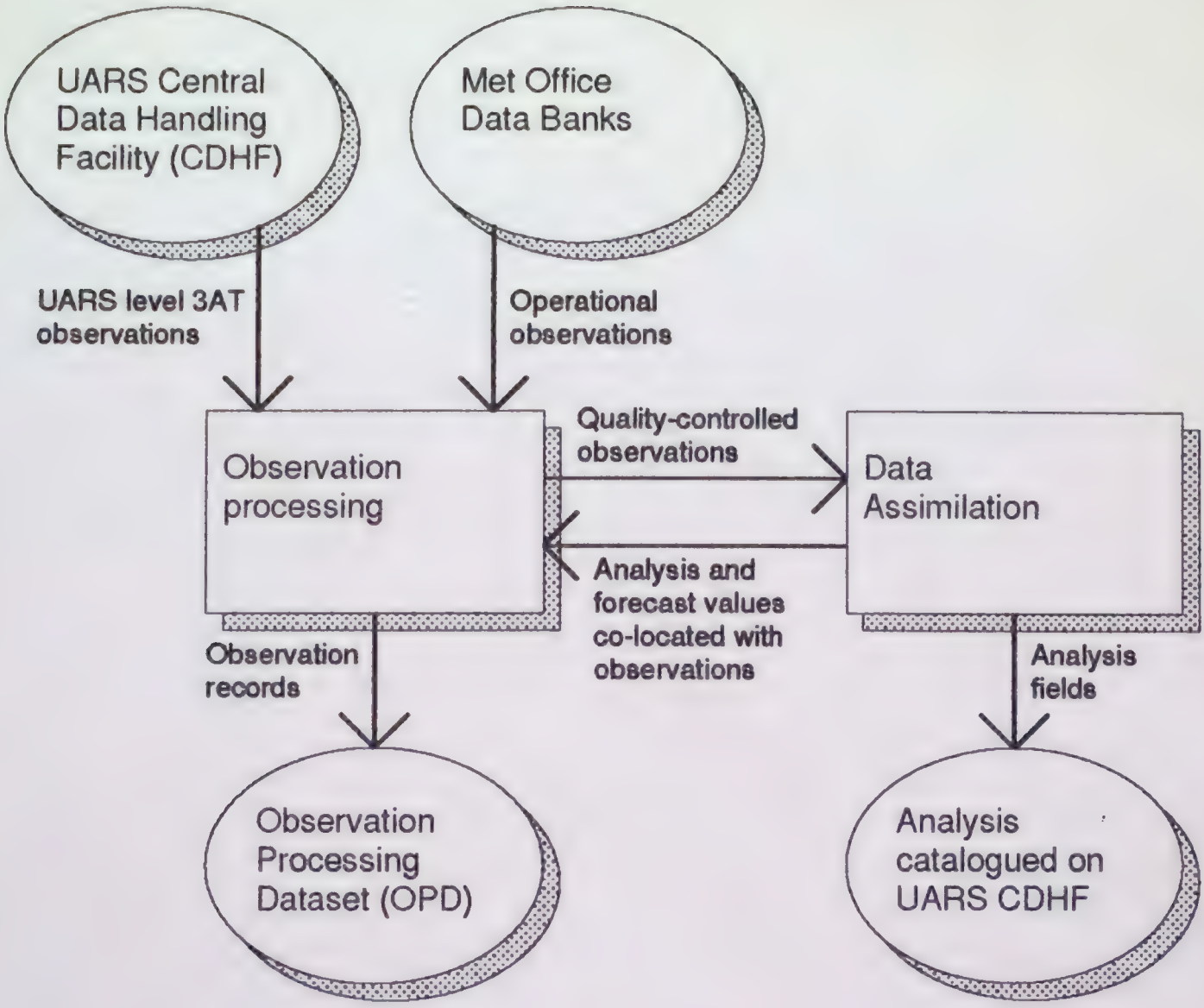
UARS Central Data Handling Facility (CDHF)
Met Office Data Banks
UARS level 3AT observations
Operational observations
Observation processing
Quality-controlled observations
Data Assimilation
Analysis and forecast values co-located with observations
Observation records
Analysis fields
Observation Processing Dataset (OPD)
Analysis catalogued on UARS CDHF

FIGURE 1

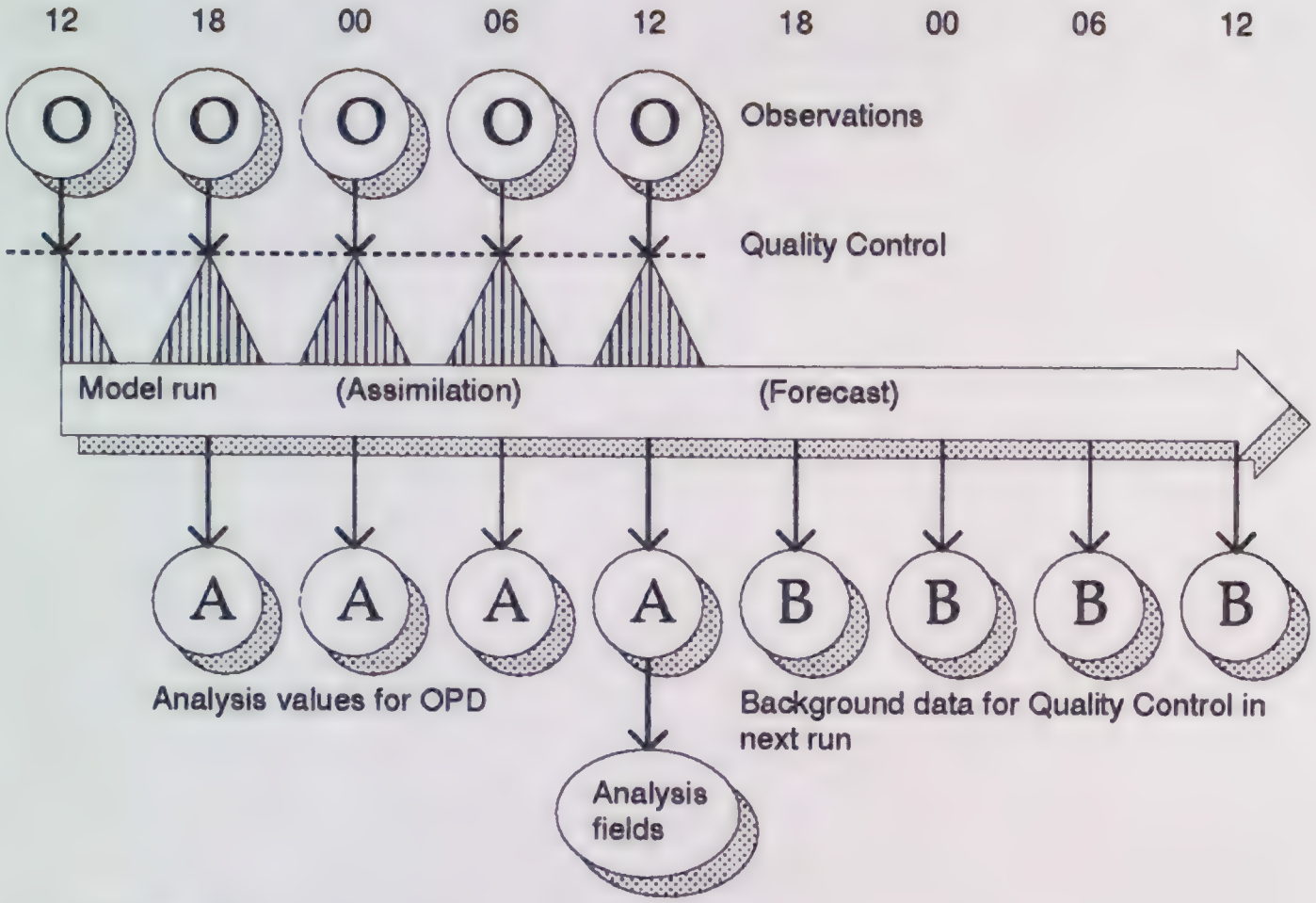
12
18
00
06
12
18
00
06
12
O
O
O
O
O
Observations
Quality Control
Model run
(Assimilation)
(Forecast)
A
A
A
A
B
B
B
B
Analysis values for OPD
Background data for Quality Control in next run
Analysis fields

FIGURE 2

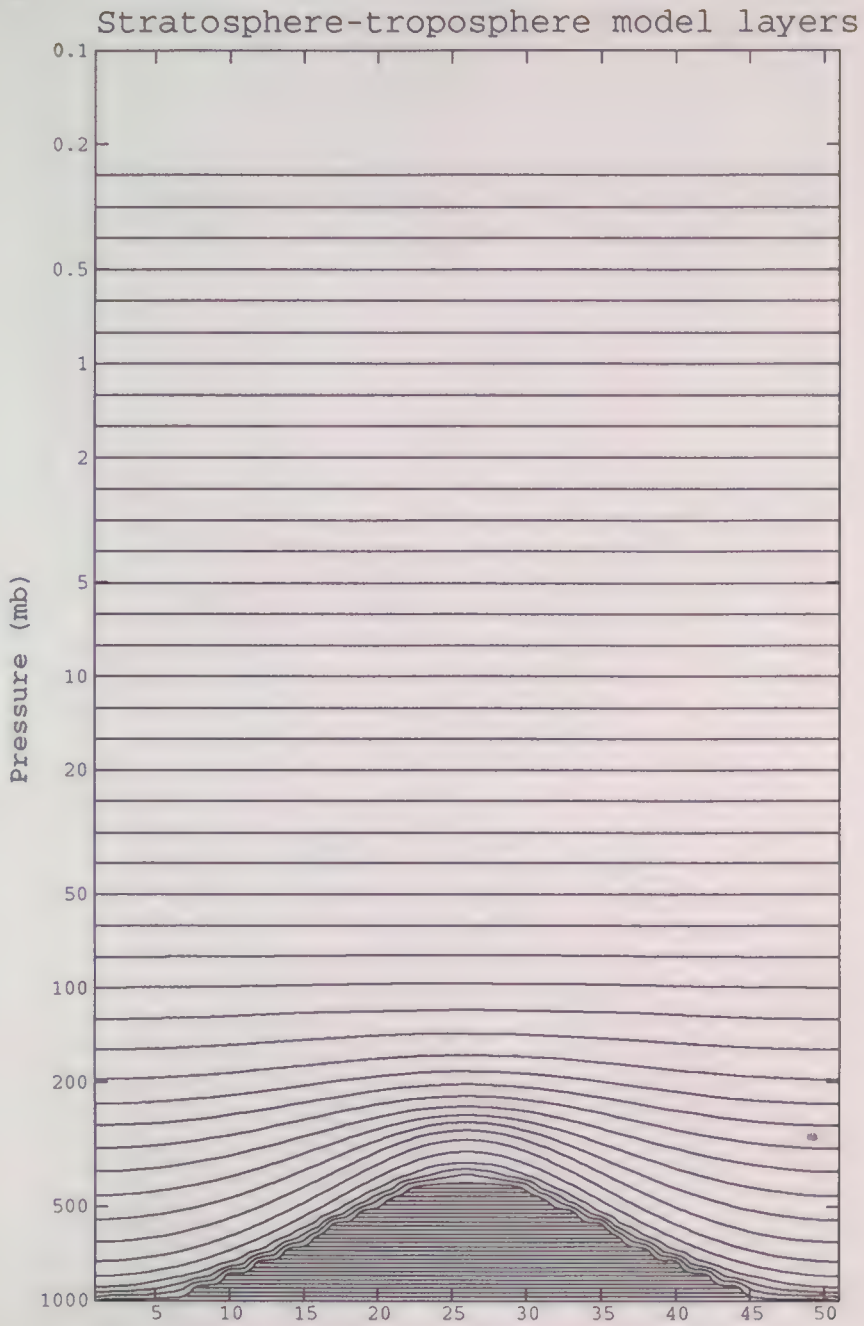
Stratosphere-troposphere model layers
Pressure (mb)
0.1
0.2
0.5
1
2
5
10
20
50
100
200
500
1000
5
10
15
20
25
30
35
40
45
50

FIGURE 3

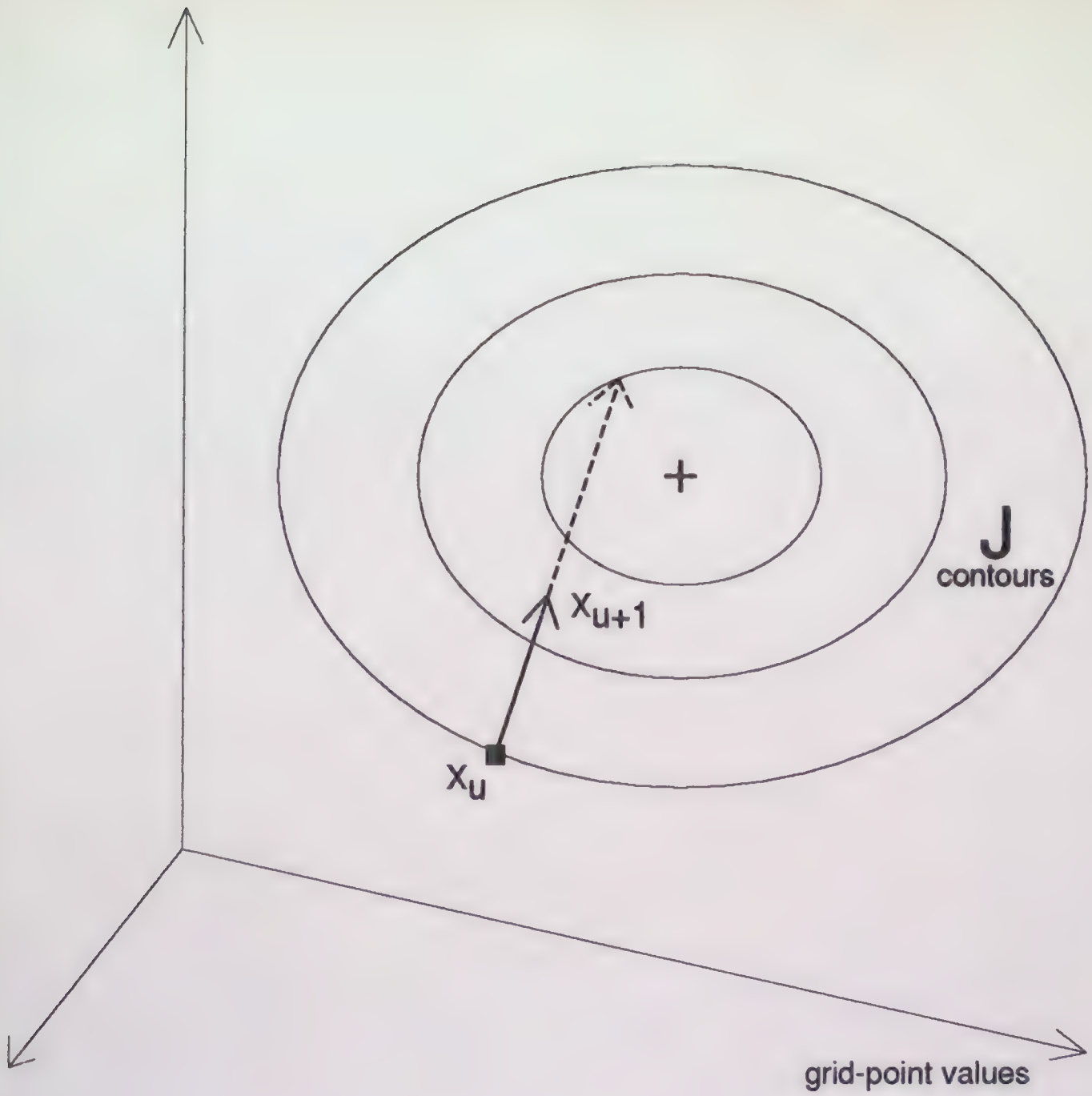

+ minimum value of J = optimum analysis <x>

----> full adjustment of x from Newton-Raphson method

——→ adjustment scaled by step-size λ

FIGURE 4

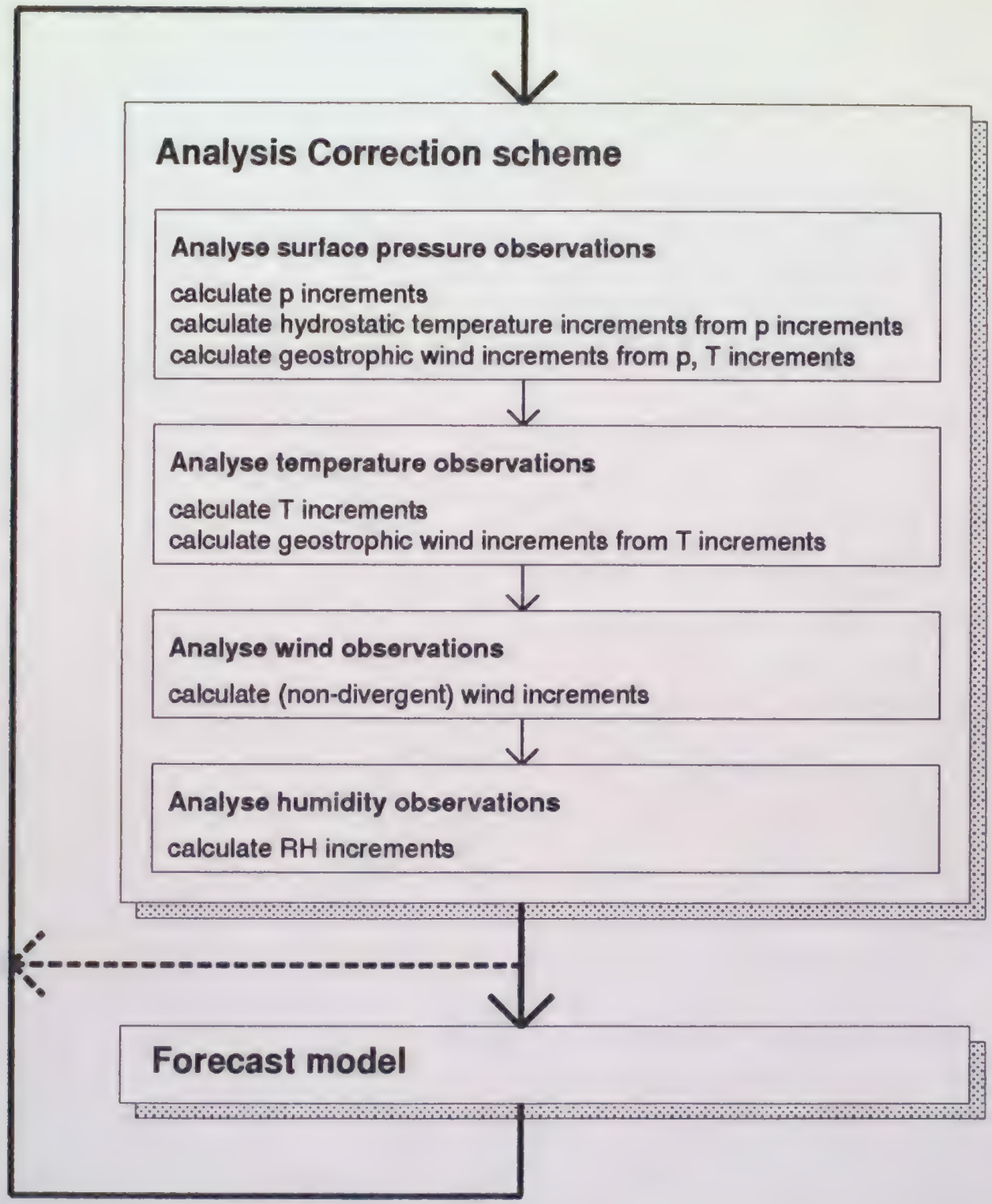
Analysis Correction scheme
Analyse surface pressure observations
calculate p increments
calculate hydrostatic temperature increments from p increments
calculate geostrophic wind increments from p, T increments
Analyse temperature observations
calculate T increments
calculate geostrophic wind increments from T increments
Analyse wind observations
calculate (non-divergent) wind increments
Analyse humidity observations
calculate RH increments
Forecast model

FIGURE 5

Fig. 6

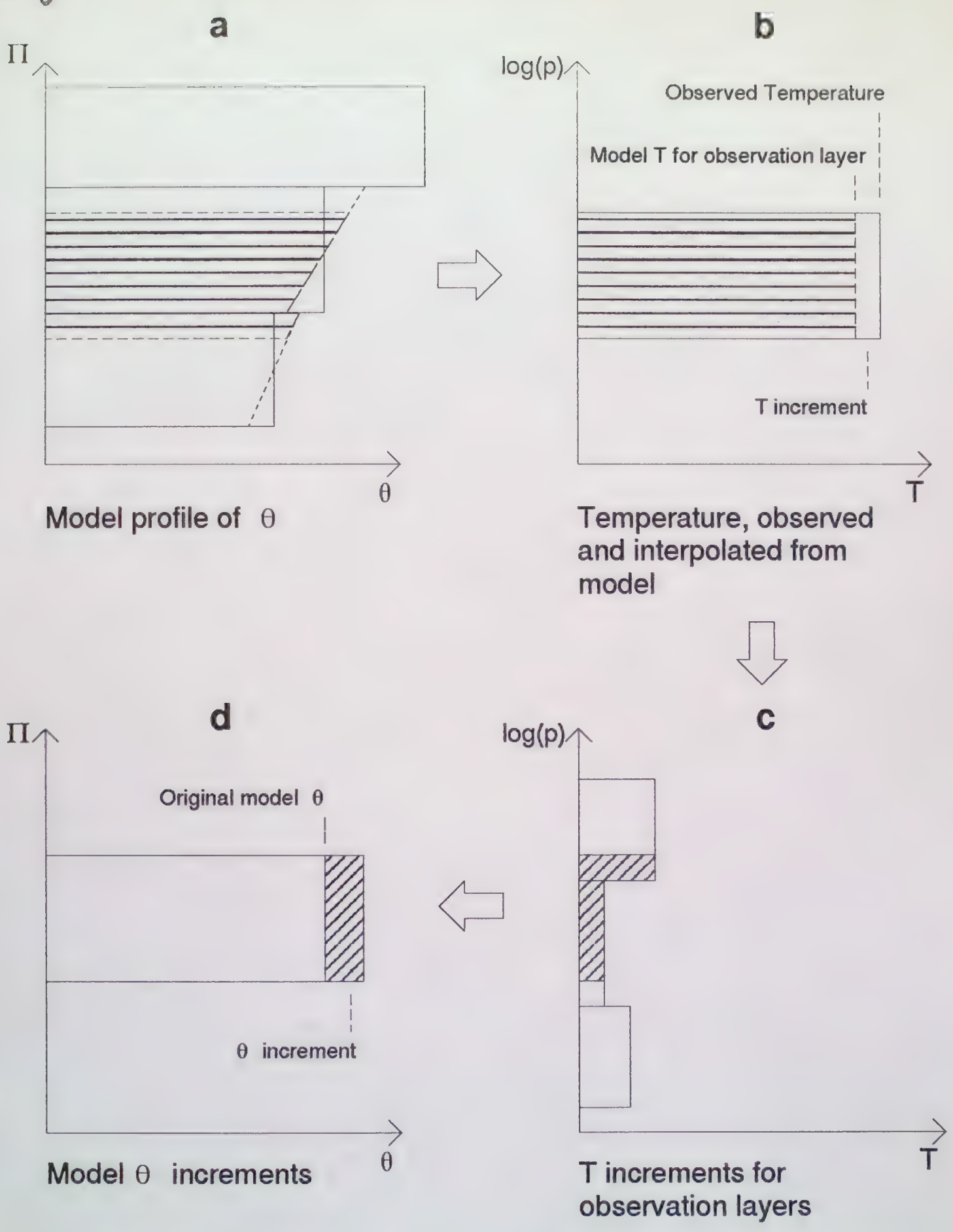
a
Π
θ
Model profile of θ
b
log(p)
Observed Temperature
Model T for observation layer
T increment
T
Temperature, observed and interpolated from model
c
log(p)
T
T increments for observation layers
d
Π
Original model θ
θ increment
θ
Model θ increments

UKMO correlative assimilation
Temperature
Valid at 12 GMT Jan 9 1992 day 120
Zonal average Experiment no.: 1006 Analysis

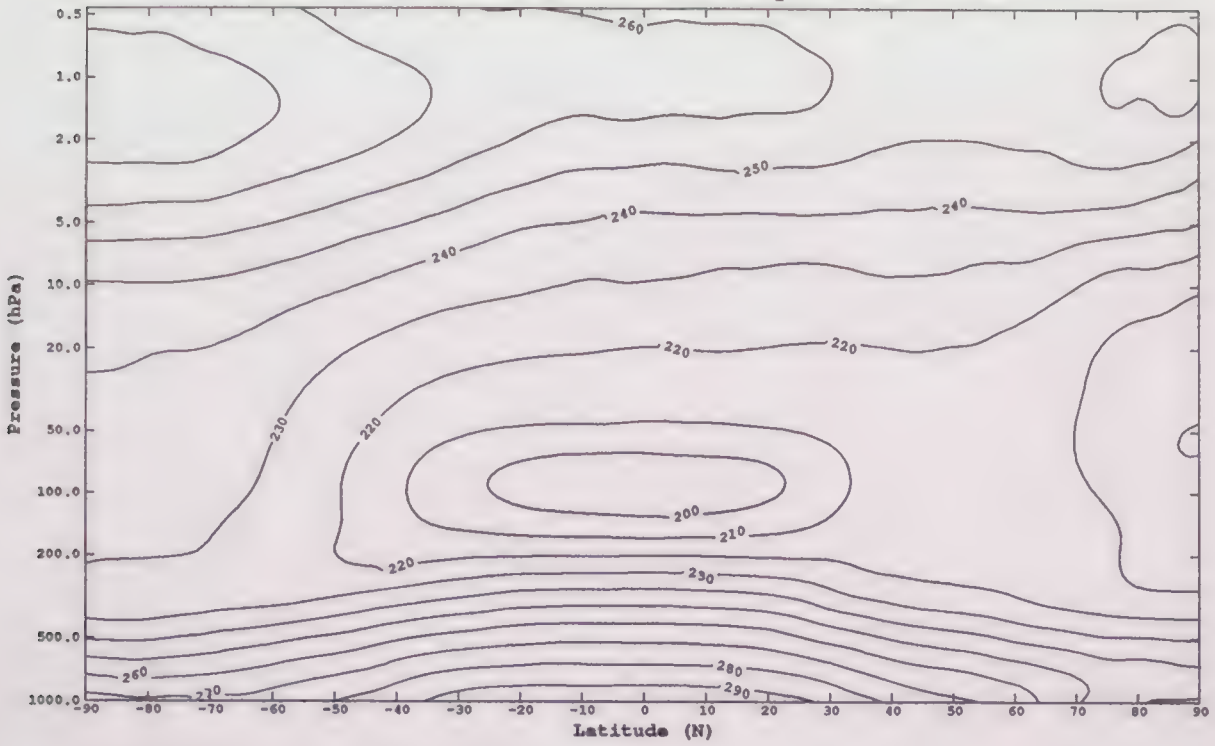

UKMO correlative assimilation minus NMC
Temperature
Valid at 12 GMT Jan 9 1992 day 120
Zonal average Experiment no.: 1006 Analysis

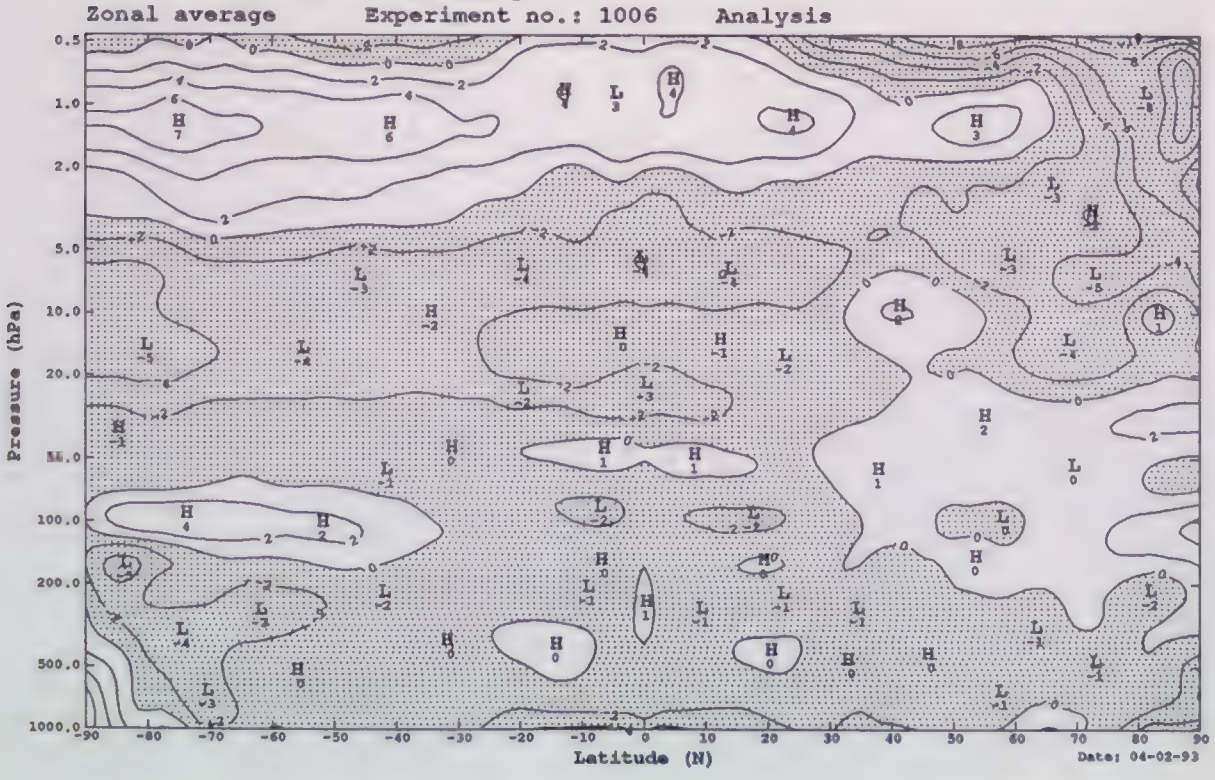

FIGURE 7

UKMO Correlative Analysis
Temperature
Valid at 12 GMT Jan 9 1992 day 120
Level: 100 hPa Experiment no.: 1006 Analysis

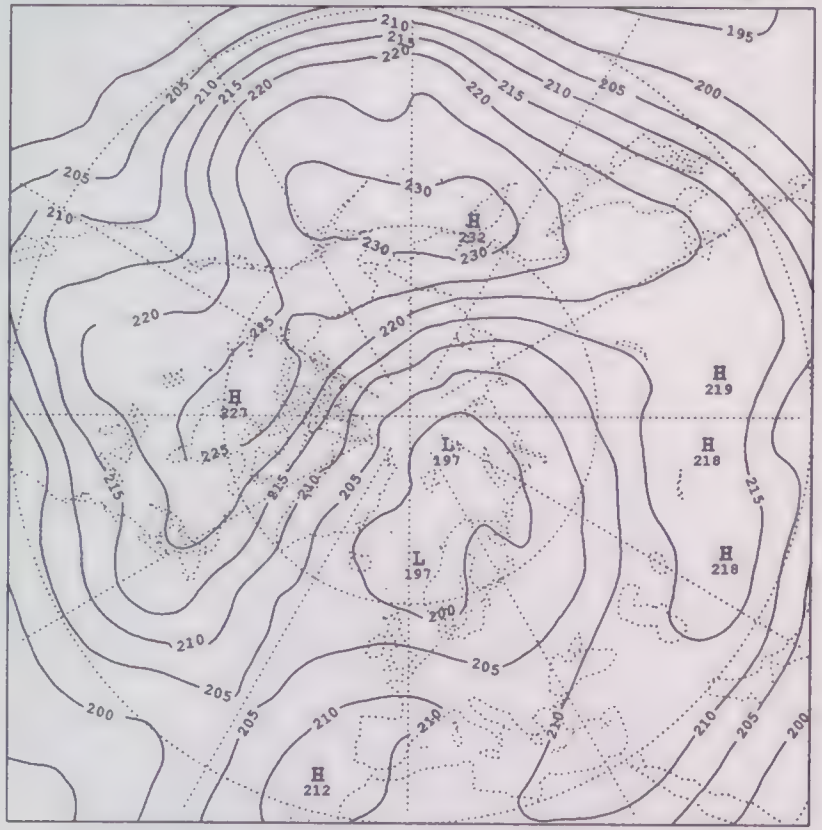

NMC analysis
Temperature
Valid at 12 GMT Jan 9 1992 day 120
Level: 100 hPa

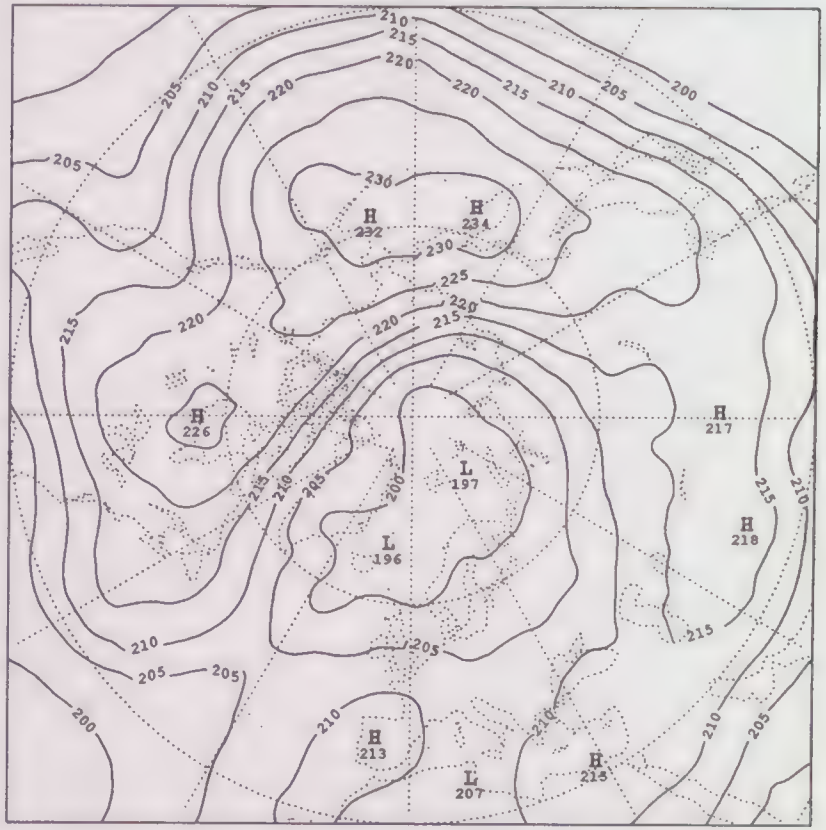

FIGURE 8

UKMO Correlative Analysis
Temperature
Valid at 12 GMT Jan 9 1992 day 120
Level: 10.0 hPa Experiment no.: 1006 Analysis

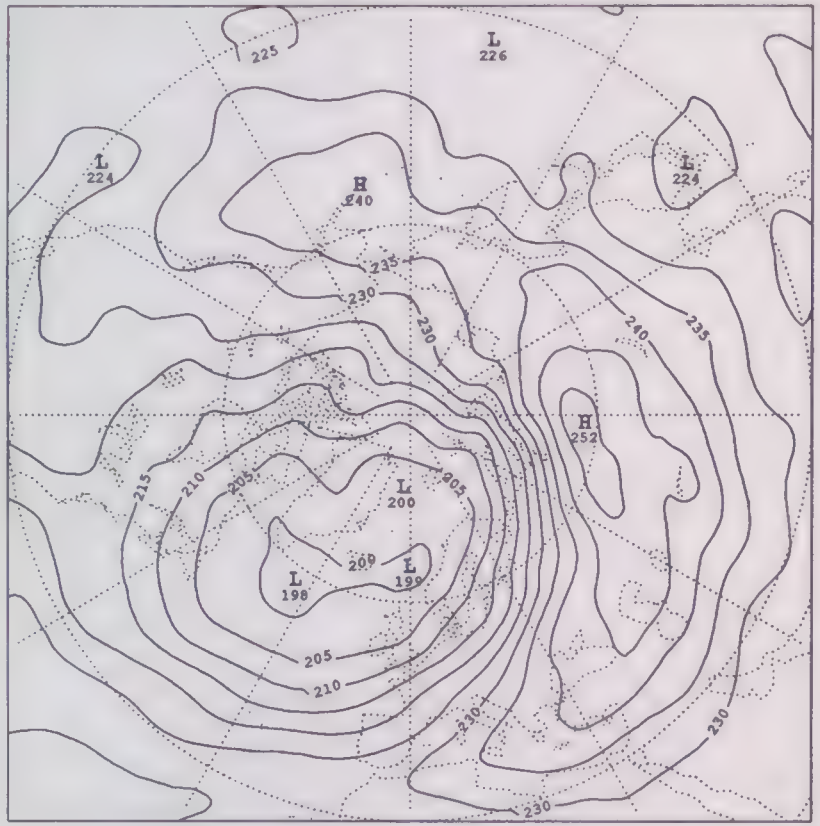

NMC analysis
Temperature
Valid at 12 GMT Jan 9 1992 day 120
Level: 10.0 hPa

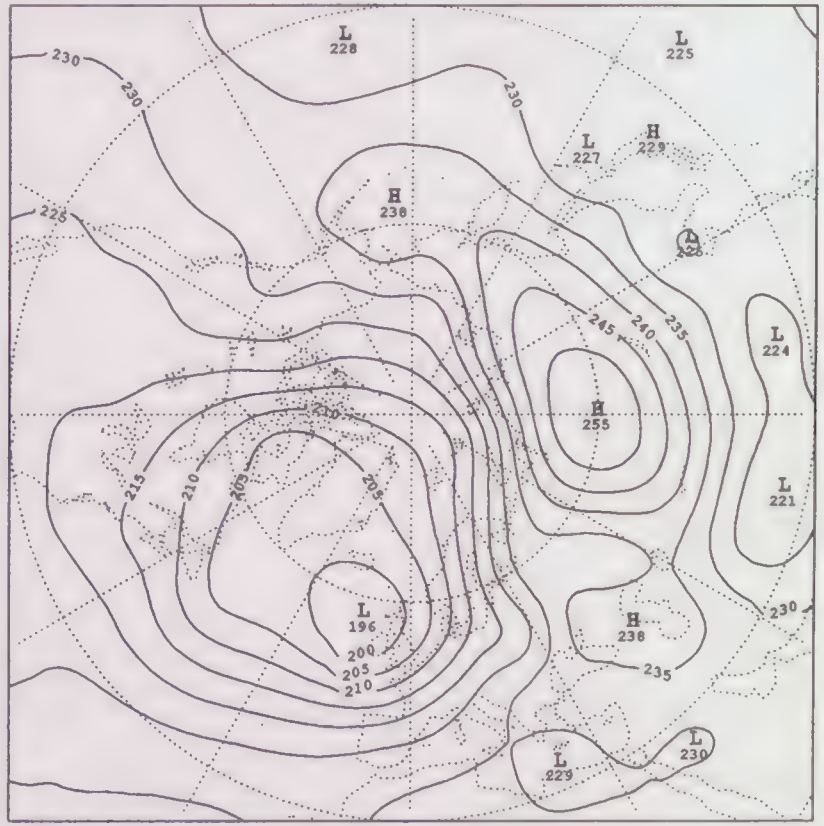

FIGURE 9

UKMO Correlative Analysis
Temperature
Valid at 12 GMT Jan 9 1992 day 120
Level: 1.00 hPa Experiment no.: 1006 Analysis

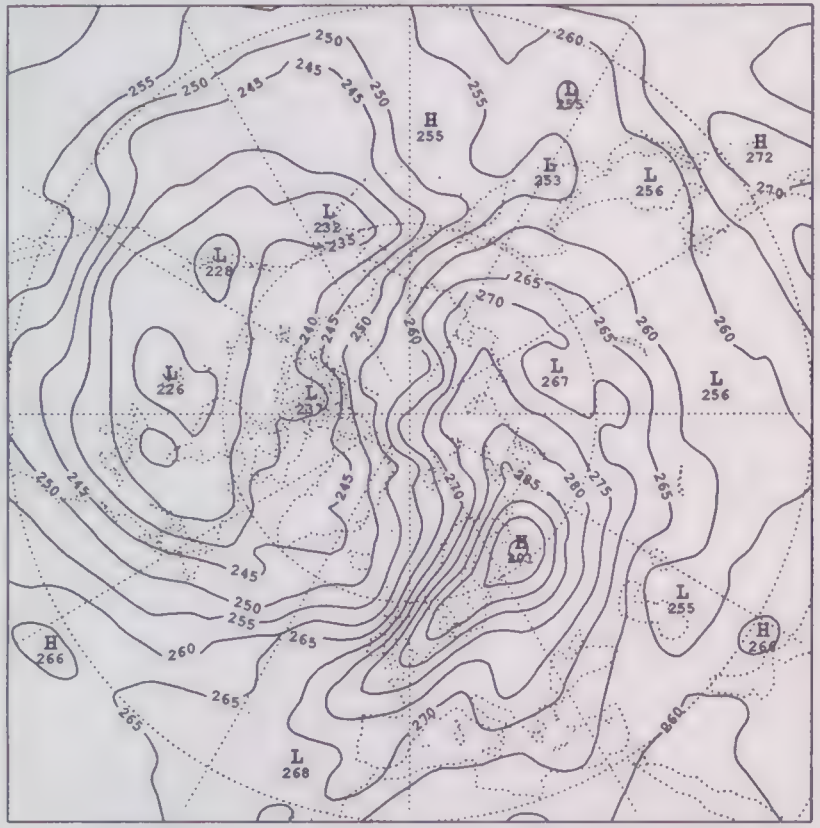

NMC analysis
Temperature
Valid at 12 GMT Jan 9 1992 day 120
Level: 1.00 hPa

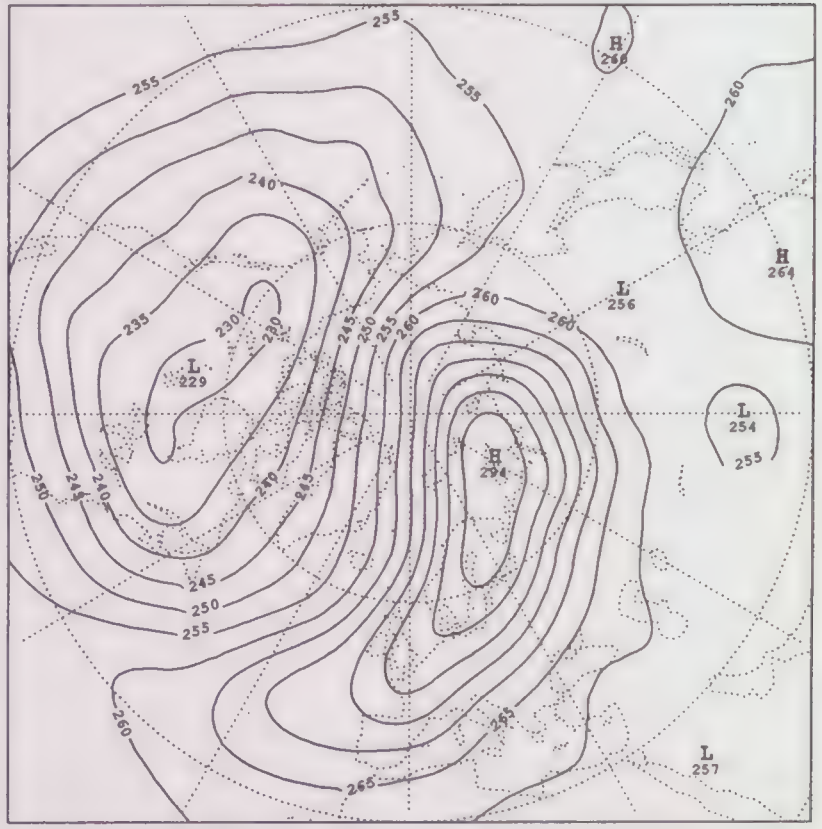

FIGURE 10

UKMO Correlative Analysis
Temperature
Valid at 12 GMT Jan 9 1992 day 120
Level: 10.0 hPa Experiment no.: 1006 Analysis

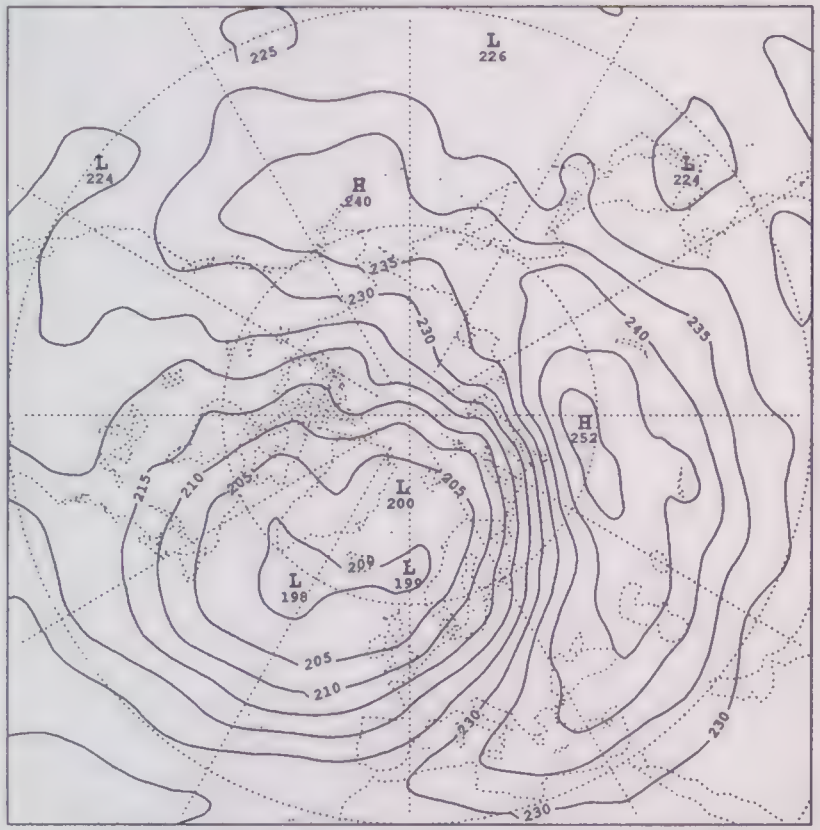

UKMO Analysis minus NMC
Temperature
Valid at 12 GMT Jan 9 1992 day 120
Level: 10.0 hPa Experiment no.: 1006 Analysis

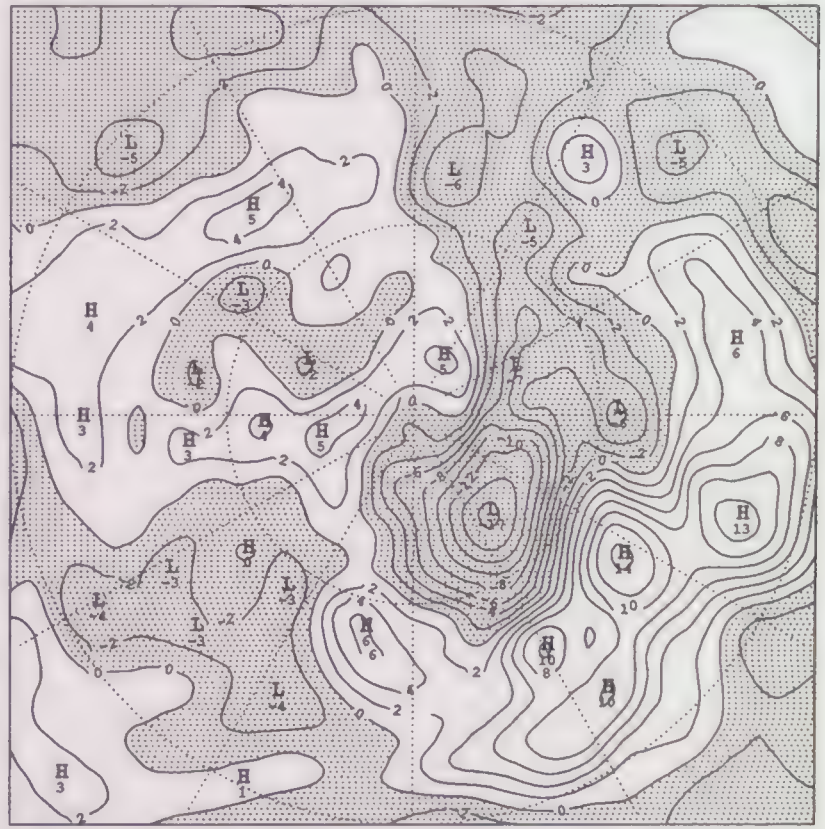

FIGURE 11

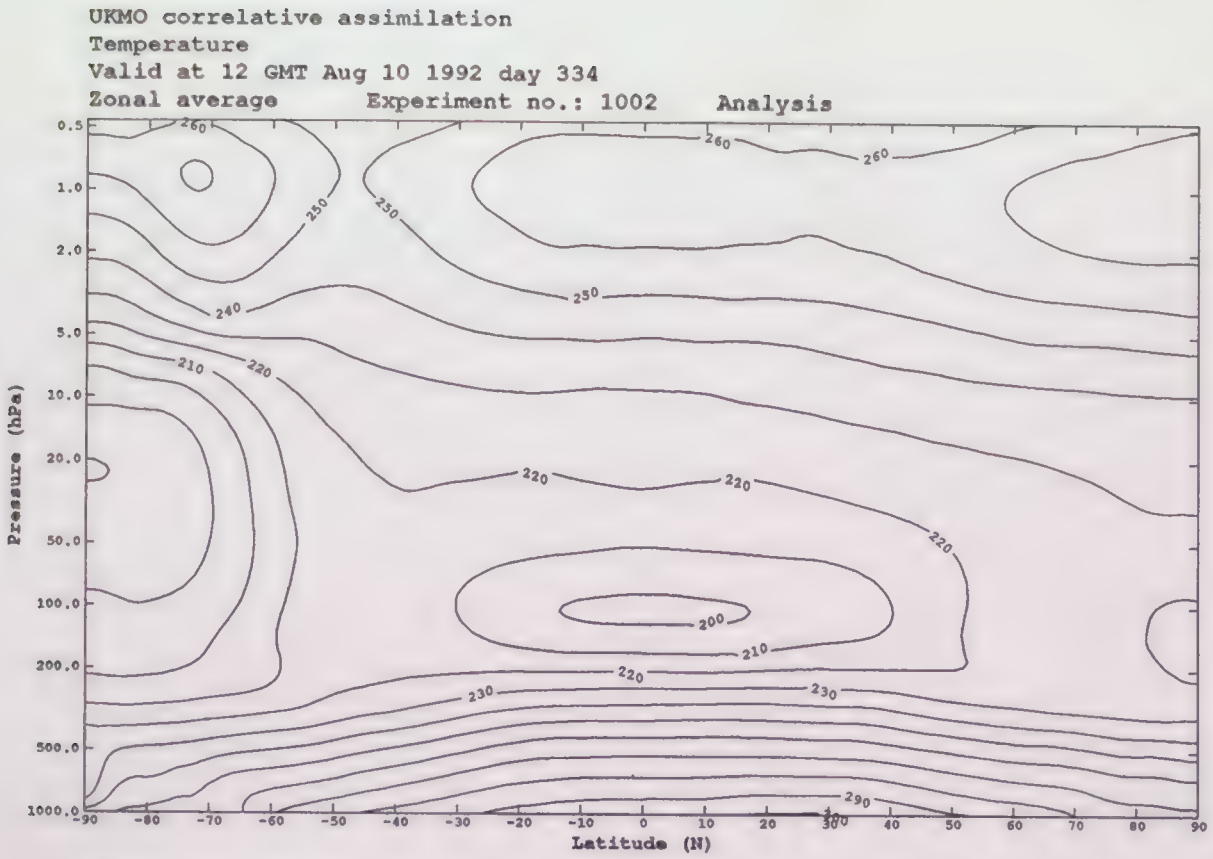
UKMO correlative assimilation
Temperature
Valid at 12 GMT Aug 10 1992 day 334
Zonal average Experiment no.: 1002 Analysis
Pressure (hPa)
Latitude (N)

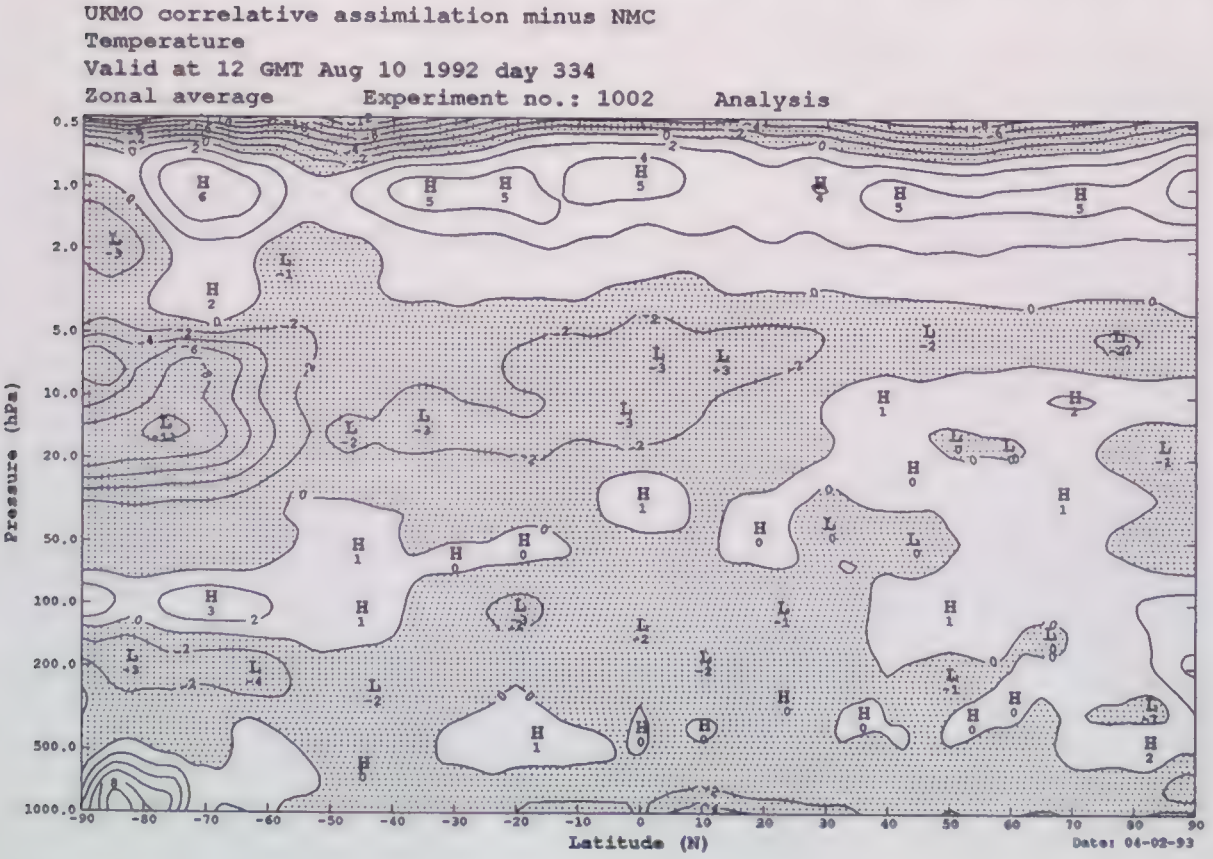
UKMO correlative assimilation minus NMC
Temperature
Valid at 12 GMT Aug 10 1992 day 334
Zonal average Experiment no.: 1002 Analysis
Pressure (hPa)
Latitude (N)
Date: 04-02-93

FIGURE 12

UKMO Correlative Analysis
Temperature
Valid at 12 GMT Aug 10 1992 day 334
Level: 10.0 hPa Experiment no.: 1002 Analysis

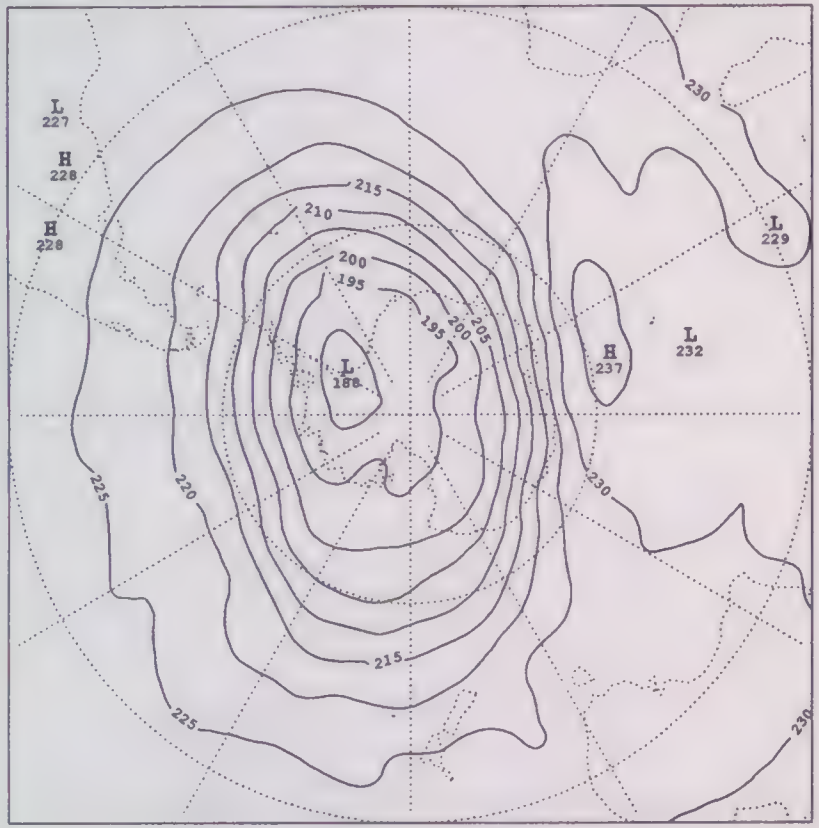

UKMO Analysis minus NMC
Temperature
Valid at 12 GMT Aug 10 1992 day 334
Level: 10.0 hPa Experiment no.: 1002 Analysis

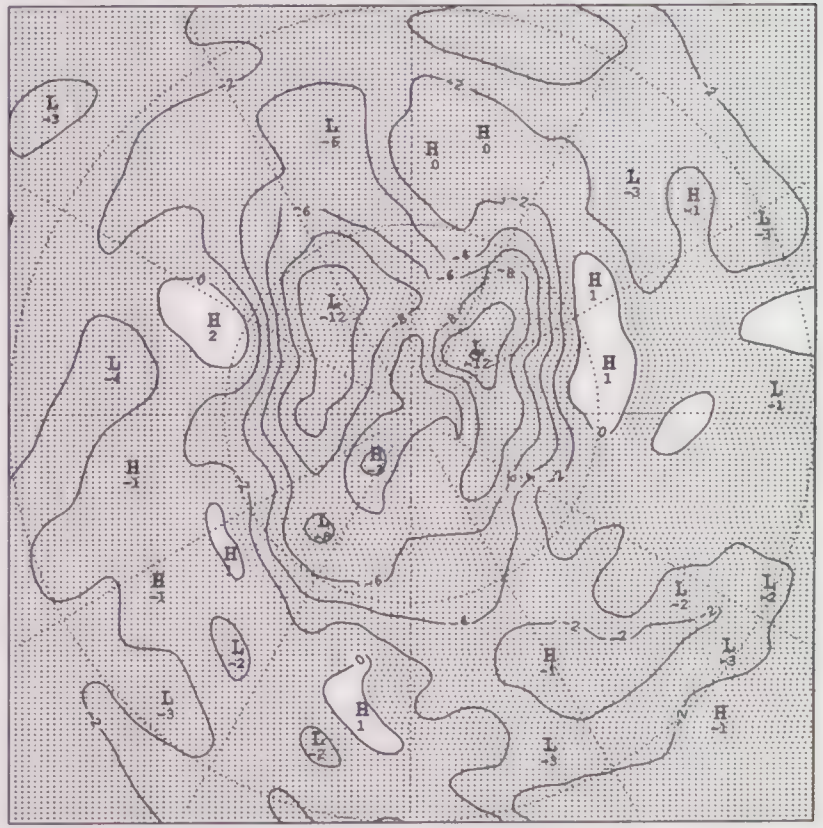

FIGURE 13

UKMO Correlative Analysis
Temperature
Valid at 12 GMT Aug 10 1992 day 334
Level: 10.0 hPa Experiment no.: 1002 Analysis

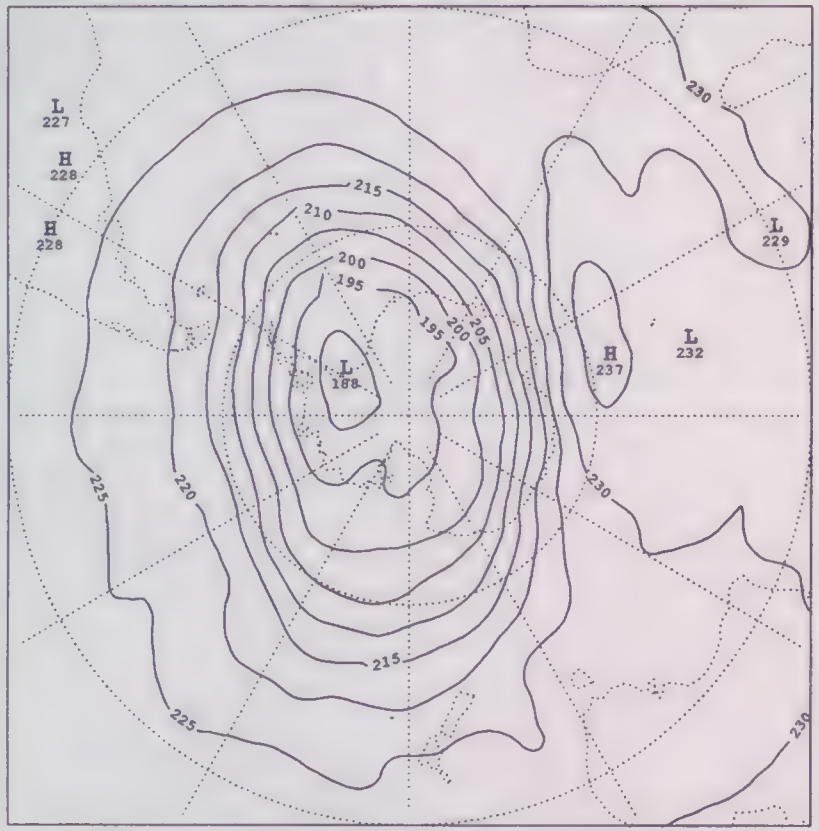

UKMO Analysis minus ECMWF
Temperature
Valid at 12 GMT Aug 10 1992 day 334
Level: 10.0 hPa Experiment no.: 1002 Analysis

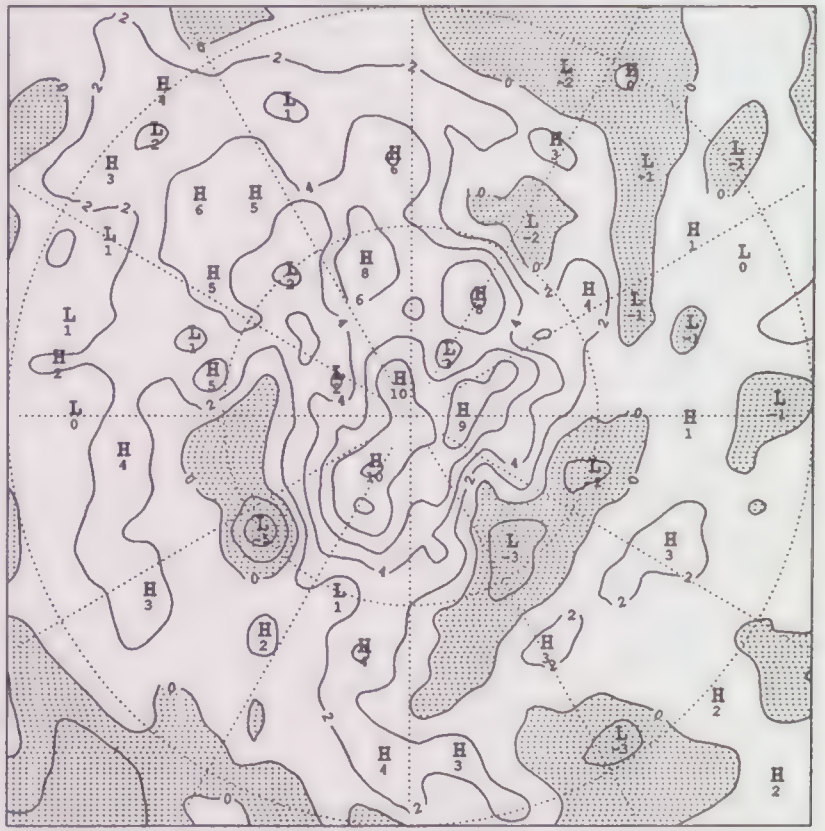

FIGURE 14

Fig 15a

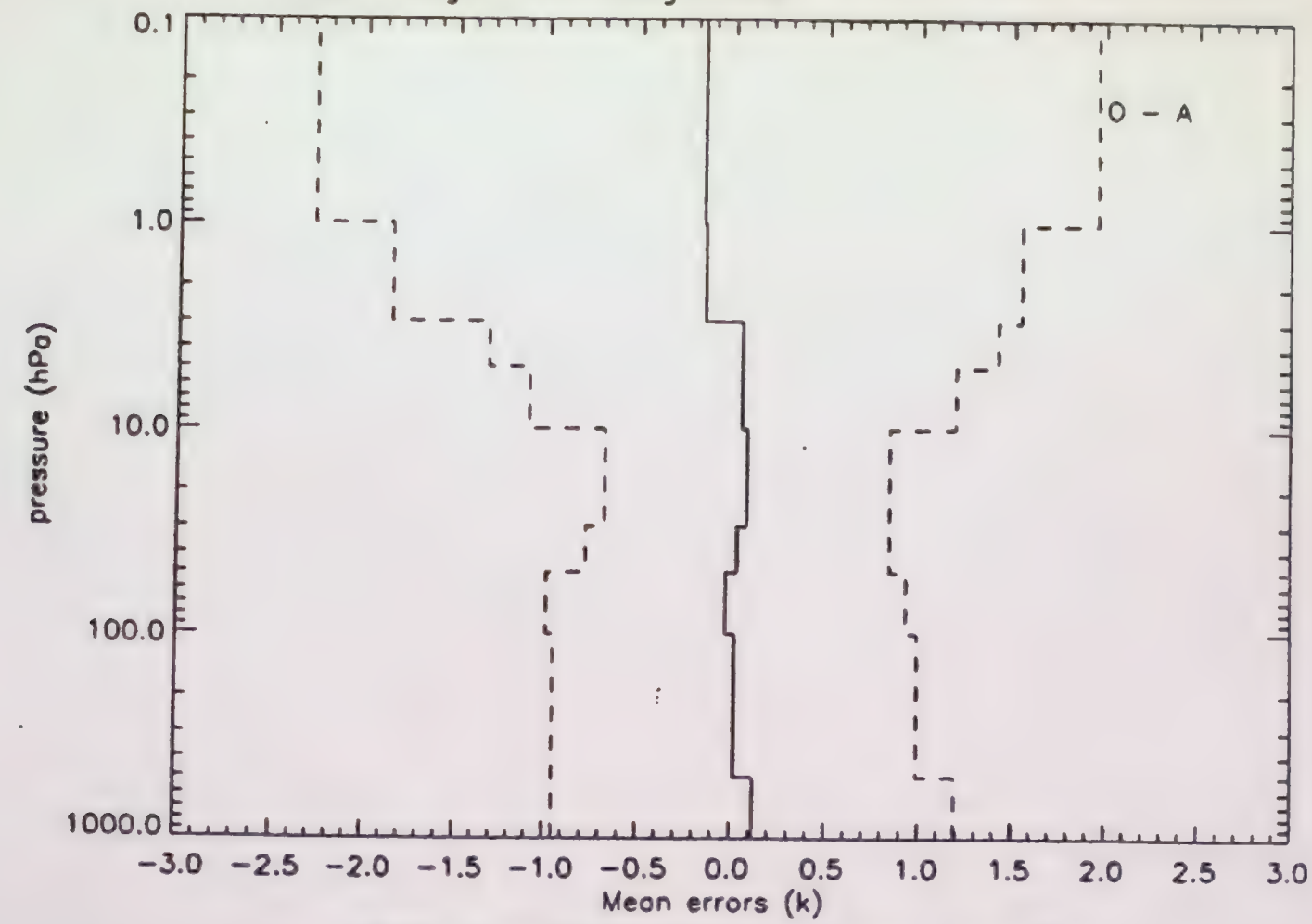
UKMO Assimilation temperatures : satellite
Region : 90.0N to 90.0S ; 180.0W to 180.0E
Date : 12gmt 10th Aug 1992
O - A
pressure (hPa)
0.1
1.0
10.0
100.0
1000.0
-3.0 -2.5 -2.0 -1.5 -1.0 -0.5 0.0 0.5 1.0 1.5 2.0 2.5 3.0
Mean errors (k)

15b

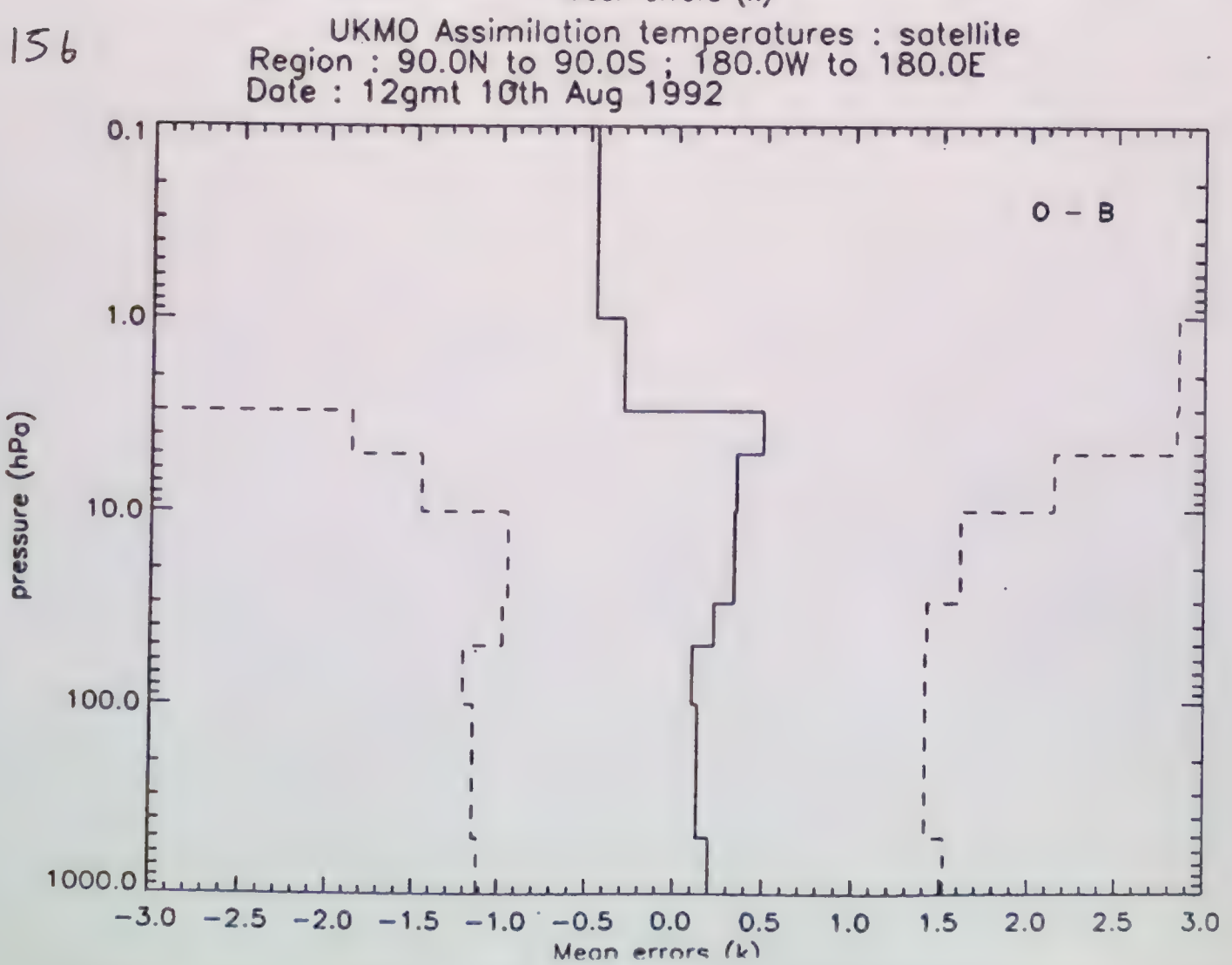
UKMO Assimilation temperatures : satellite
Region : 90.0N to 90.0S ; 180.0W to 180.0E
Date : 12gmt 10th Aug 1992
O - B
pressure (hPa)
0.1
1.0
10.0
100.0
1000.0
-3.0 -2.5 -2.0 -1.5 -1.0 -0.5 0.0 0.5 1.0 1.5 2.0 2.5 3.0
Mean errors (k)

Fig. 16a

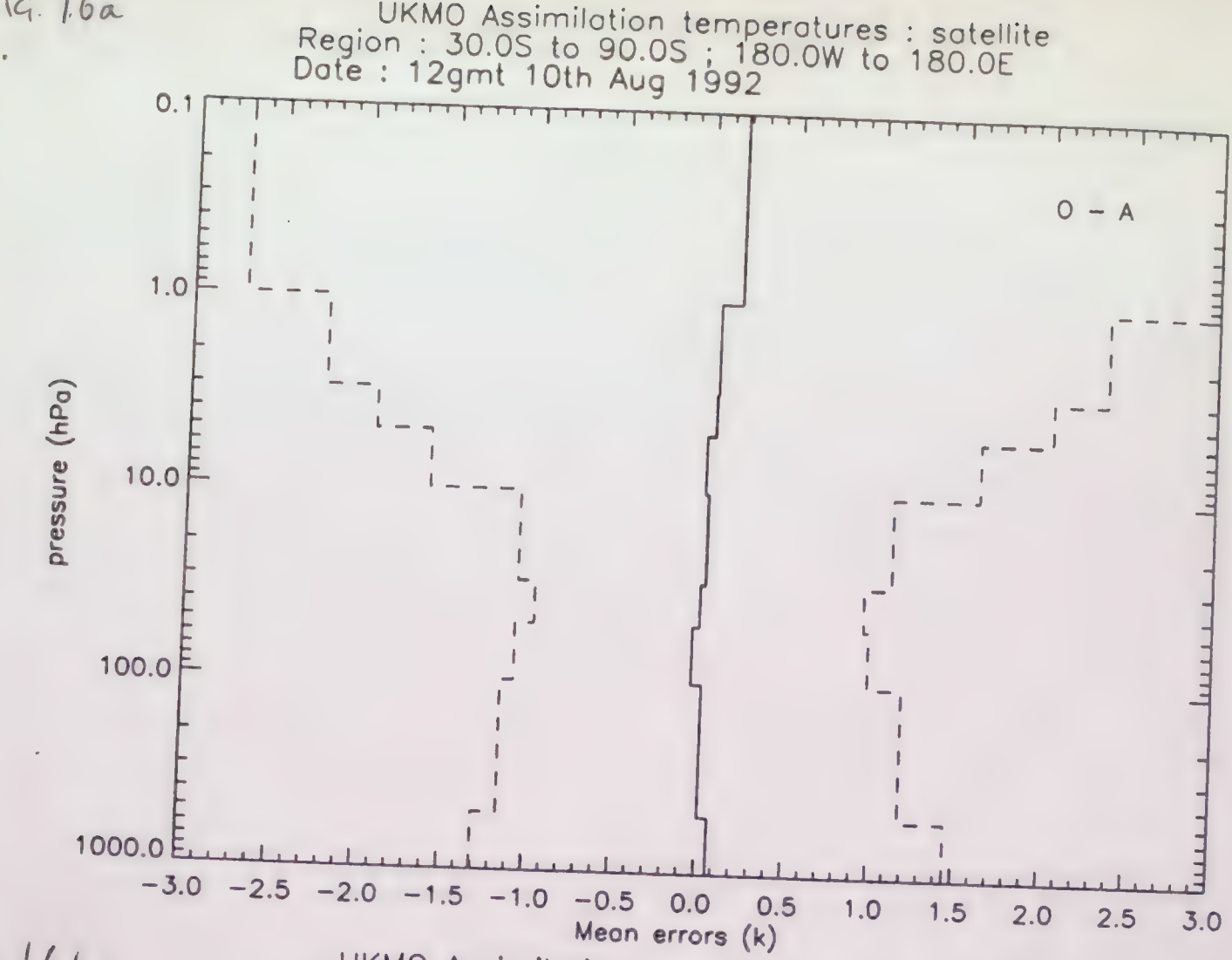
UKMO Assimilation temperatures : satellite
Region : 30.0S to 90.0S ; 180.0W to 180.0E
Date : 12gmt 10th Aug 1992
O - A
pressure (hPa)
0.1
1.0
10.0
100.0
1000.0
-3.0 -2.5 -2.0 -1.5 -1.0 -0.5 0.0 0.5 1.0 1.5 2.0 2.5 3.0
Mean errors (k)

166

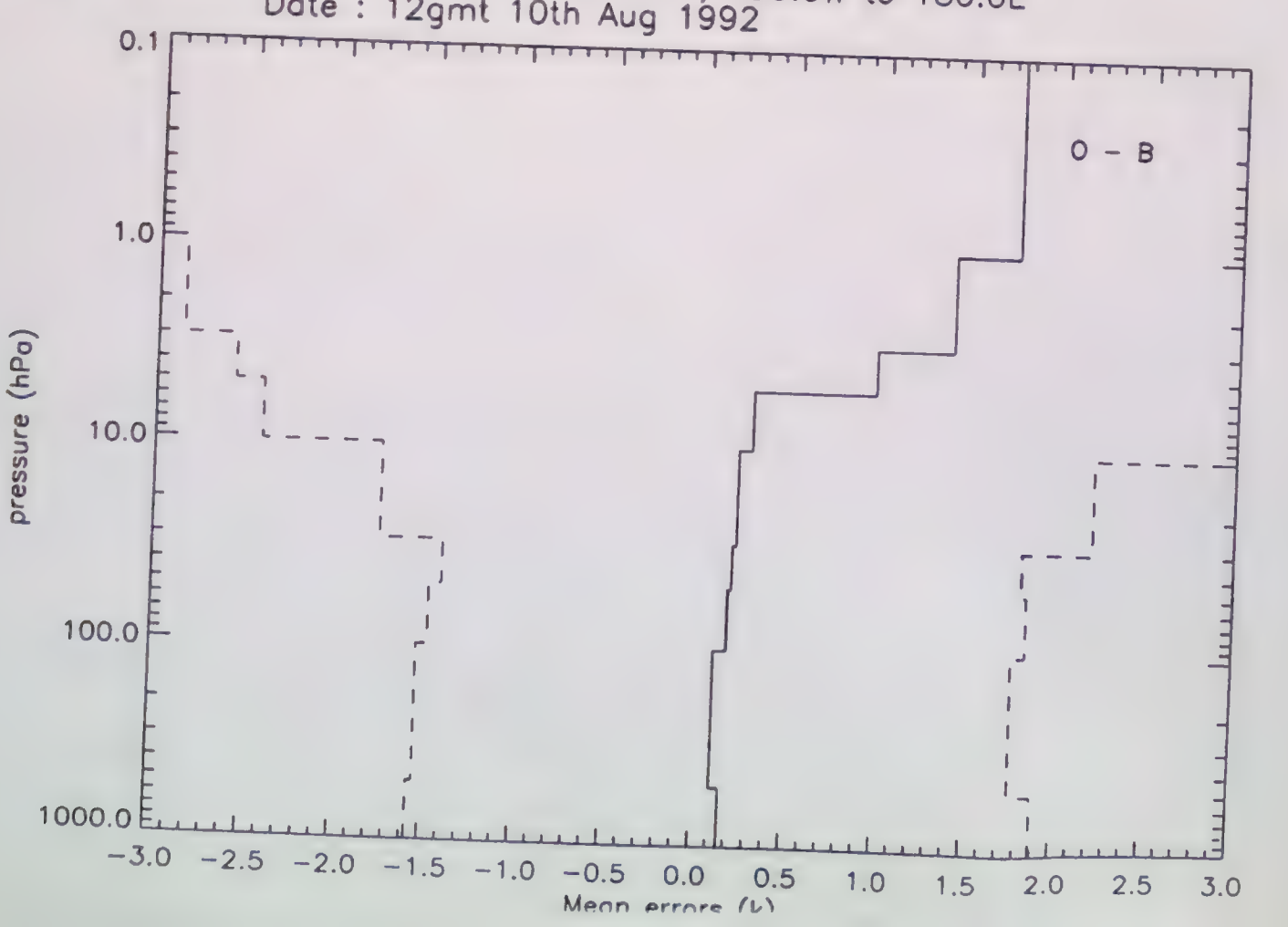
UKMO Assimilation temperatures : satellite
Region : 30.0S to 90.0S ; 180.0W to 180.0E
Date : 12gmt 10th Aug 1992
O - B
pressure (hPa)
0.1
1.0
10.0
100.0
1000.0
-3.0 -2.5 -2.0 -1.5 -1.0 -0.5 0.0 0.5 1.0 1.5 2.0 2.5 3.0
Mean errors (k)

UARS correlative assimilation
Temperature
Valid at 12 GMT Jan 27 1992 day 138
Experiment no.: 1004 Analysis

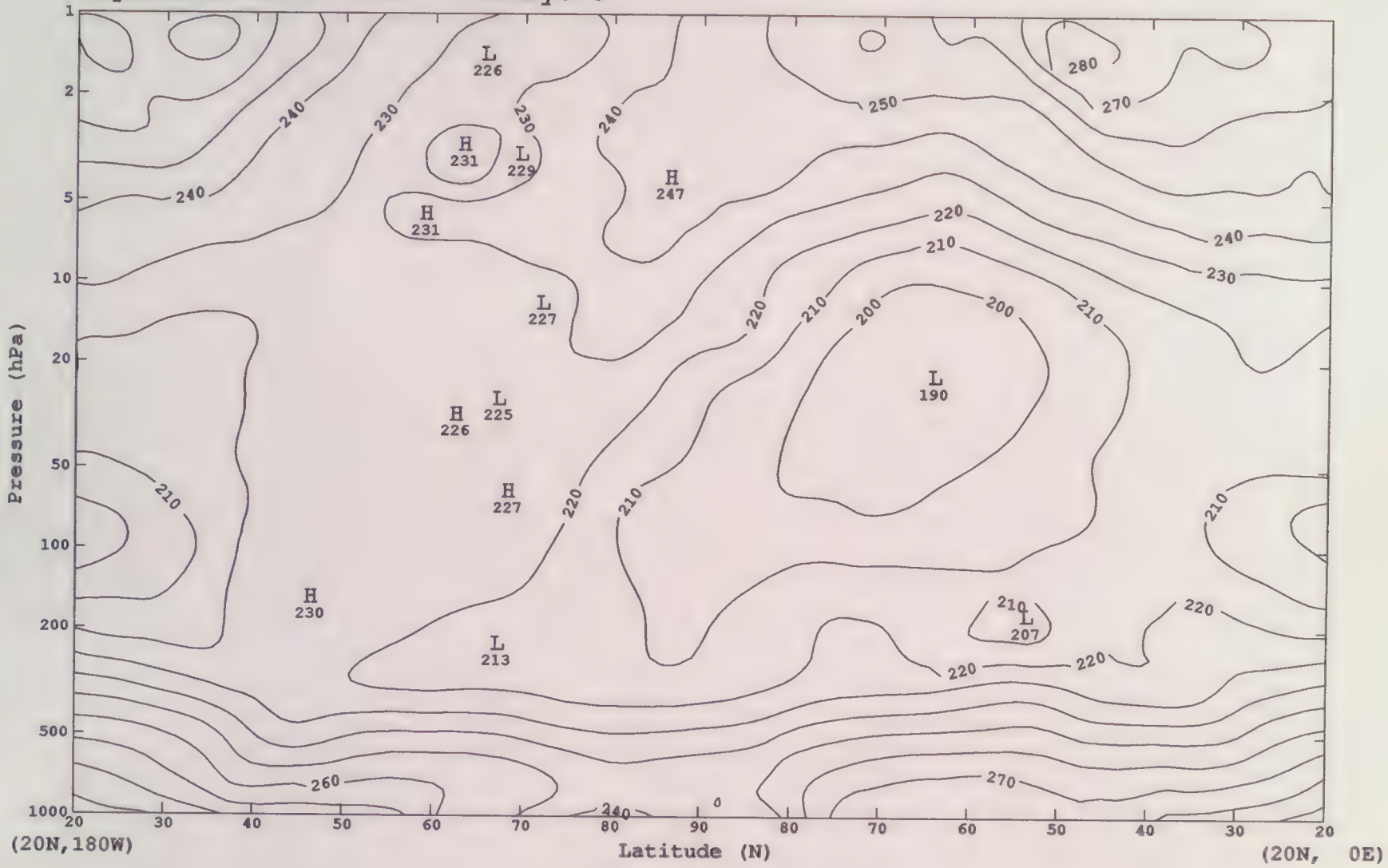

FIGURE 17

UARS correlative assimilation
Wind (perpendicular to cross-section)
Valid at 12 GMT Jan 27 1992 day 138
Experiment no.: 1004 Analysis

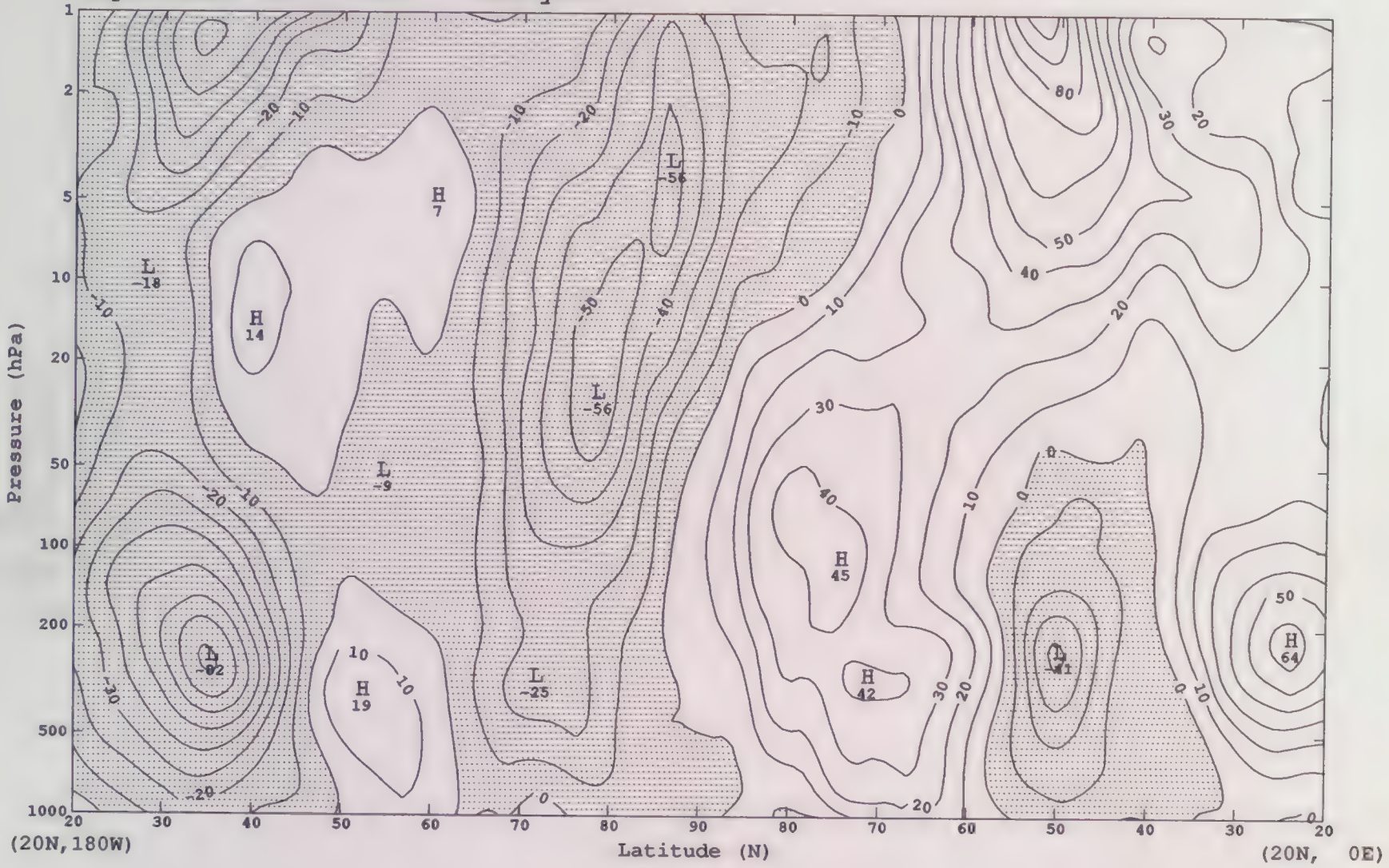

FIGURE 18

UKMO Correlative Analysis
Potential vorticity
Valid at 12 GMT Jan 27 1992 day 138
Level: 315 K

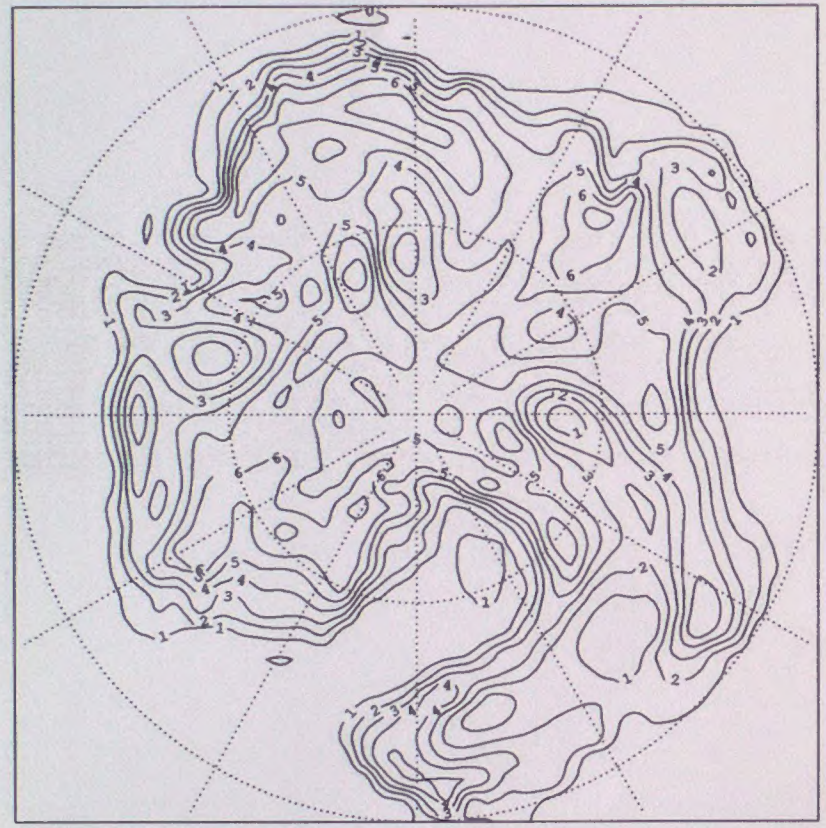

FIGURE 19

UKMO Correlative Analysis
Potential vorticity
Valid at 12 GMT Jan 27 1992 day 138
Level: 520 K

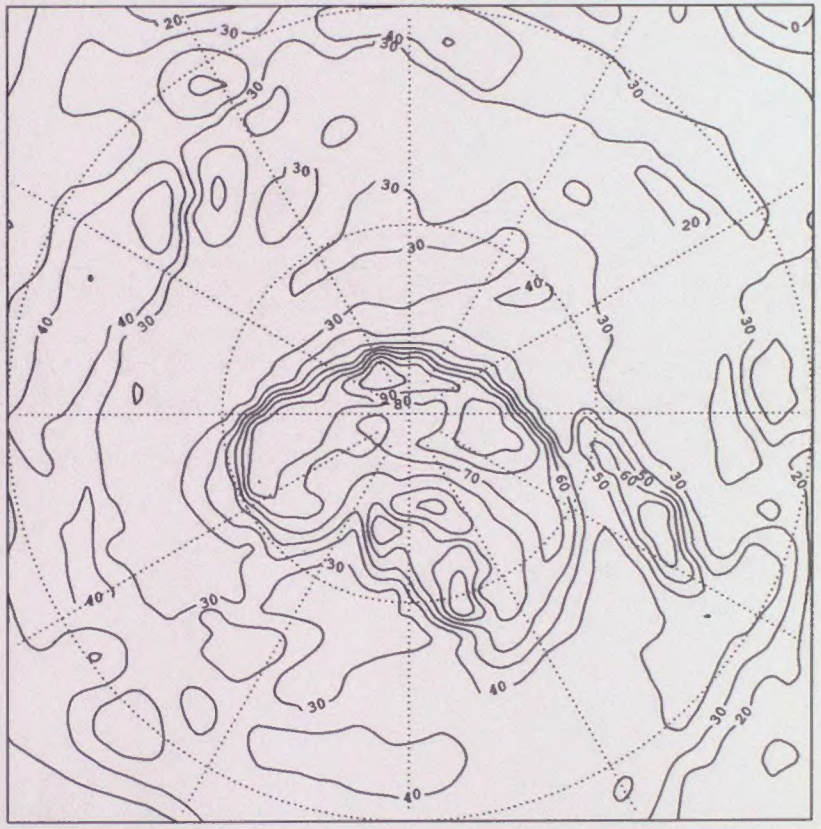

FIGURE 20

CLIMATE RESEARCH TECHNICAL NOTES

CRTN 1	Oct 1990	Estimates of the sensitivity of climate to vegetation changes using the Penman-Monteith equation. P R Rowntree
CRTN 2	Oct 1990	An ocean general circulation model of the Indian Ocean for hindcasting studies. D J Carrington
CRTN 3	Oct 1990	Simulation of the tropical diurnal cycle in a climate model. D P Rowell
CRTN 4	Oct 1990	Low frequency variability of the oceans. C K Folland, A Colman, D E Parker and A Bevan
CRTN 5	Dec 1990	A comparison of 11-level General Circulation Model Simulations with observations in the East Sahel. K Maskell
CRTN 6	Dec 1990	Climate Change Prediction. J F B Mitchell and Qing-cun Zeng
CRTN 7	Jan 1991	Deforestation of Amazonia - modelling the effects of albedo change. M F Mylne and P R Rowntree
CRTN 8	Jan 1991	The role of observations in climate prediction and research. D J Carson
CRTN 9	Mar 1991	The greenhouse effect and its likely consequences for climate change. D J Carson
CRTN 10	Apr 1991	Use of wind stresses from operational N.W.P. models to force an O.G.C.M. of the Indian Ocean. D J Carrington
CRTN 11	Jun 1991	A new daily Central England Temperature series, 1772-1991. D E Parker, T P Legg and C K Folland
CRTN 12	Jul 1991	Causes and predictability of Sahel rainfall variability. D P Rowell, C K Folland, K Maskell, J A Owen, M N Ward
CRTN 13	Jul 1991	Modelling changes in climate due to enhanced CO_2, the role of atmospheric dynamics, cloud and moisture. C A Senior, J F B Mitchell, H Le Treut and Z-X Li

CLIMATE RESEARCH TECHNICAL NOTES

CRTN 14	Sep 1991	Sea temperature bucket models used to correct historical SST data in the Meteorological Office. C K Folland
CRTN 15	Aug 1991	Modelling climate change, and some potential effects on agriculture in the U.K. P R Rowntree, B A Callander and J Cochrane
CRTN 16	Aug 1991	The Boreal Forests and Climate G Thomas and P R Rowntree
CRTN 17	Aug 1991	Development of a Stratosphere-Troposphere Data Assimilation System. R Swinbank.
CRTN 18	Sep 1991	A study of asynchronous coupling using a simple climate model. M K Davey.
CRTN 19	Sep 1991	The Oceanic Carbon Cycle. N K Taylor
CRTN 20	Nov 1991	Worldwide ocean-atmosphere surface fields in Sahel wet and dry years using provisionally corrected surface wind data. M N Ward
CRTN 21	Dec 1991	Coupled tropical ocean global atmosphere models at the UKMO. M K Davey, C Gordon, S Ineson and S Lawrence
CRTN 22	Dec 1991	Empirical parameterisation of tropical ocean-atmosphere coupling. M Allen, M K Davey, D L T Anderson and P D Killworth
CRTN 23	Feb 1992	The temporal evolution of Equatorial Currents in the Indian Ocean D L T Anderson, D J Carrington, R A Corry and C Gordon
CRTN 24	Feb 1992	Stratospheric analyses provided by the U.K. Meteorological Office M J Bailey, A O'Neill and V D Pope
CRTN 25	Feb 1992	Modelling interannual variability in the Indian Ocean using momentum fluxes from the UKMO and ECMWF operational weather analyses. D L T Anderson and D J Carrington

CLIMATE RESEARCH TECHNICAL NOTES

CRTN 26	Mar 1992	A GCM simulation of the impact of Amazonian deforestation on climate using an improved canopy representation J Lean and P R Rowntree
CRTN 27	Mar 1992	The parameterization of rainfall interception in GCMs A J Dolman and D Gregory
CRTN 28	Jun 1992	Development of worldwide marine data eigenvectors since 1985 A W Colman
CRTN 29	Jun 1992	A tropical ocean model with reduced physics M K Davey
CRTN 30	Jun 1992	International Temperature Workshop, Boulder, Colorado, USA, 16 January 1992 Edited by D E Parker
CRTN 31	Jul 1992	Simulation of clear-sky outgoing longwave radiation over the oceans using operational analyses A Slingo and M J Webb
CRTN 32	Sep 1992	A prediction of the transient response of climate J M Murphy
CRTN 33	Nov 1992	LEPS scores for assessing climate model simulations and long-range forecasts. C K Folland
CRTN 34	Jan 1993	Stratospheric Data Assimilation System Guide Editer: R Swinbank
CRTN 35	Mar 1993	A Stratosphere-Troposphere Data Assimilation System R Swinbank and A O'Neill